LEVEL

DEPARTMENT OF THE AIR FORCE

AIR UNIVERSITY (ATC)

AIR FORCE INSTITUTE OF TECHNOLOGY

Wright-Patterson Air Force Base, Ohio

81 2 01 010

14 JAN 1981

Analysis of Dye Degradation Effects on Output
Energy of the Pulsed Organic Dye Laser,

Master . THESIS.

AFIT/GEP/PH/80D-1   Alan J. Briding
                        Capt   USAF

Dec 80

105

Approved for public release; distribution unlimited.

012205

ANALYSIS OF DYE DEGRADATION EFFECTS ON OUTPUT ENERGY

OF THE PULSED ORGANIC DYE LASER

THESIS

Presented to the Faculty of the School of Engineering

of the Air Force Institute of Technology

Air University

in Partial Fulfillment of the

Requirements for the Degree of

Master of Science

by

Alan J. Briding

Capt   USAF

Graduate Engineering Physics

December 1980

Preface

The Air Force Avionics Laboratory at Wright-Patterson AFB, Ohio has conducted and sponsored extensive research into the lasing properties of Kiton Red S. One of the important conclusions of this research was that a multiplier effect was causing a logarithmic decay in pulse energy that was sssociated with a linear rate of KRS degradation.

At this point it seemed advisable to try to explain the phenomena with a theoretical analysis. My thesis modeled the KRS laser and derived a method of predicting what effect several degradation mechanisms could have on its performance. My next step was to try to obtain the necessary information from the wealth of data recorded by the previous studies to test the model and then use it to explain the multiplier effect. Unfortunately, the specific data required to arrive at conclusive results was not available, through no lack of thoroughness on my predecessors' part. Most of the requirements for the analysis were not readily foreseeable, and are included in my recommendations for further research.

I would like to express my appreciation to Capt. David Hardin for his assistance in designing the computer programs, to Dr. Robert Schwerzel of the Battelle Laboratories in Columbus for his help in determining values for the model parameters, to my thesis typist Jill Rueger whose expertise and consideration were invaluable, and to my thesis advisor, Dr. Ernest Dorko, who blended the proper amounts of assistance and supervision into an enjoyable project.

Contents

Contents

List of Figures

List of Figures (continued)

List of Tables

Notation

S_i	ith singlet energy level
T_i	ith triplet energy level
E_i	ith energy level
N_i	ith level population density
N_T	T_1 triplet level population density
P_i	ith energy level population density (normalized)
a_{ij}	spontaneous radiation and radiationless transition rates combined
n	cavity photon population

$k_{S_1 S_0}$	$S_1 \to S_0$ internal conversion rate
$k_{S_1 T_1}$	$S_1 \to T_1$ intersystem crossing rate
$k_{T_1 S_0}$	$T_1 \to S_0$ intersystem crossing rate
k_{QS}	singlet quenching rate constant
k_{QT}	triplet quenching rate constant
$k_{QS(RP)}$	rate constant for singlet quenching by the reaction product
$k_{QT(RP)}$	rate constant for triplet quenching by the reaction product
Q_S	concentration of singlet quencher
Q_T	concentration of triplet quencher
$Q_{S(RP)}$	concentration of the reaction product $= c_{RP}$

τ_F	fluorescence lifetime
$\tau_{F(R)}$	radiative fluorescence lifetime
$\tau_{F(NR)}$	nonradiative fluorescence lifetime
τ_P	phosphorescence lifetime

$\tau_{P(R)}$ — radiative phosphorescence lifetime

$\tau_{P(NR)}$ — nonradiative phosphorescence lifetime

τ_C — cavity photon lifetime

τ_M — photon cavity lifetime due to frontal mirror transmission only

α — absorption coefficient at the lasing wavelength

η — quantum pump efficiency

η' — modified quantum pump efficiency

Π — pump absorption factor

ϕ — quantum efficiency of fluorescence

λ_L — wavelength of a lasing photon

ν_L — frequency of lasing photon

ν_P — frequency of pump photon

γ — laser gain coefficient

ϵ — molar extinction coefficient

ϵ_P — molar extinction coefficient at the pump wavelength

ϵ_D — molar extinction coefficient at the lasing wavelength of the dye

ϵ_{RP} — molar extinction coefficient of the reaction product at the lasing wavelength

δ_S — ratio of the $S_0 \rightarrow S_1$ extinction coefficient to the $S_1 \rightarrow S_2$ extinction coefficient at the lasing wavelength

δ_T — ratio of the $S_0 \rightarrow S_1$ extinction coefficient to the $T_1 \rightarrow T_2$ extinction coefficient at the lasing wavelength

$\sigma_{A(D)}$ — pump absorption cross section for the dye

$\sigma_{A(RP)}$ — pump absorption cross section for the reaction product

ρ — number of pump photons absorbed per second by the medium

ρ_0 — number of pump photons transmitted per second in the initial beam

Notation (continued)

$N_{2,TH}$ threshold population for lasing

$W_{P,TH}$ threshold pump power

P_{laser} power output of a laser

$W(t)$ pumping function

W_{max} peak value of the Gaussian pumping pulse

T half-width at half-height of the pumping pulse

L length of the dye solution traversed by a photon during a single pass through the laser cavity

ℓ distance between mirrors in the laser cavity

n_D index of refraction of the dye solution

R_1 reflectivity of the frontal cavity mirror

R_2 reflectivity of the rear cavity mirror

c_D concentration of the dye

c_{RP} concentration of the reaction product $= Q_{S(RP)}$

Abstract

The dominant excitation and relaxation mechanisms found in dye molecules are discussed and are then incorporated into a model for the xanthene dye laser. Rate equations for this model are presented which include terms that account for excited state singlet absorption and triplet absorption. The system of rate equations are solved using the steady-state approximation to derive equations for the threshold pump and output power of the laser.

The output power and threshold pump power equations are modified to include variables that allow the following effects of dye degradation to be examined: dye concentration reduction, reaction product absorption of pump radiation, reaction product absorption of lasing radiation, and singlet quenching by the reaction products. Theoretical values based on available experimental data are derived for these variables. A computer program is used to integrate the output power of the laser over the duration of a flashlamp pulse to compute the pulse energy.

The computer program presented is designed to determine how the output energy of the laser decreases over the course of repeated pulsing as the specific degradation effects increase with the increase in the reaction product. The results obtained from the theoretical analysis are compared to experimental data that describe a logarithmic decay of output energy associated with a linear decay in the dye concentration (the multiplier effect). Of those mechanisms examined, the absorption of lasing radiation appears to be the most effective factor that could contribute to the multiplier effect; however, it cannot account for the magnitude of the multiplier effect without considering additional

mechanisms operating simultaneously. Further experimentation is recom-
mended to obtain specific data for conclusive identification of the
responsible mechanism.

I. Introduction

Background

Dye lasers are being closely examined by the Air Force for use on aircraft as sources for optical radar and other electro-optical systems. The laser must operate in the 630-670 nanometer (nm) region up to three hours without servicing. The xanthene dye Kiton Red S (KRS) is currently under investigation to determine if it is capable of meeting these standards.

The complex structure and size of laser dyes make them susceptible to photochemical dissociation into reaction products. The degradation and performance of KRS under both continuous wave (CW) and flashlamp pumping has been extensively investigated (Refs 15, 16, 20, 25). The photodissociation process has been shown to be a function of the wavelength of the irradiance. The precise mechanism appears to be extremely complex due to the formation of transient reaction products. The exact nature of the transient and final reaction products has not yet been determined (Ref 33). Two important conclusions have been reached concerning KRS: the number of dye molecules lost through degradation increases at a constant rate with the number of pulses, and an unidentified multiplier effect is operating that produces a large decrease in the pulse energy for a small increase in the amount of dye degradation (Ref 25).

Objective

The objective of this study is to perform a theoretical analysis of the KRS laser system to explain the multiplier effect. The interactions examined as possible causes are limited to absorption of the lasing

1

radiation by a reaction product, absorption of the pump radiation, and singlet quenching by a reaction product.

Assumptions

The data on the degradation rate and the pulse energy decay presented by Rabins et al. (Ref 25) are assumed to be correct. The most reliable method of measuring the amount of degradation has been under contention to some extent; the method used by Rabins based on the infrared (IR) spectra of the dye solution appears to be the most accurate technique.

Approsch and Presentation

The primary mechanisms involved with the structure and chemistry of laser dyes are described in Section II. The energy levels of the dye molecule and associated excitation and relaxation pathways are discussed: these include fluorescence and phosphorescence, thermalization, internal conversion, intersystem crossing, singlet and triplet quenching, and triplet and excited state singlet absorption. The degradation effects that the study is going to examine are then presented, and the section concludes with a brief description of several important characteristics of pulsed dye lasers.

In Section III, a model is proposed to represent the dye lsser and rate equations appropriste to this model are developed. Using the steady-state approximation the rste equstions are used to obtain equations expressing the threshold pump power and the output power of the laser.

Thefe equations sre specifically applied to the KRS dye laser in Section IV. The pulse energy is obtained by integrating the output power over the durstion of the flashlamp pulse by computer. Values for the required parameters are selected and variables are then introduced to

2

provide a means of evaluating the reaction product effects. The section

ends by presenting the results obtained from the computer analysis.

Several aspects of these results are briefly discussed in Section

V.   Conclusions and recommendations are given in Section VI.

II. Mechanics of the Dye Laser

The complex structure of organic laser dyes presents many facets to consider in understanding the lasing process. The numerous mechanisms involved and their interplay have hampered precise characterization of the dyes and have led to conflicting data in the literature. This section presents the structure and basic molecular mechanics of xanthene dyes to provide a background for the development of a workable model applicable to xanthene dye lasers.

Structure and Energy Levels of Dyes

Organic dyes are large, complex molecules that contain conjugated double bonds (Ref 31:7). These molecules can be approximated by a core and an electron cloud. The core consists of σ-bonding electrons that are well localized and do not participate in optical-wavelength transitions; the π-orbital electrons are delocalized over most of the molecule (Ref 40:31). This extended conjugated bond provides strong absorption in the visible region of the spectrum due to electronic transitions from the highest-filled bonding molecular orbital to the lowest antibonding molecular orbital ($\pi \rightarrow \pi^*$) (Refs 9:184, 31:144). The family of xanthene dyes that includes KRS and the rhodamine compounds consist of the parent xanthene compound (Figure 1) with a 9-carbon substituent that provides the variations in characteristics of the individual dyes (Ref 9:182). The structures of KRS, Rhodamine B, and Rhodamine 6G are also shown in Figure 1 (Ref 13:3885). These compounds have the π-electron cloud extending over the nitrogen atoms (Ref 25:5). This π-electron cloud can be considered as a one-dimensional particle in a box to quantum-
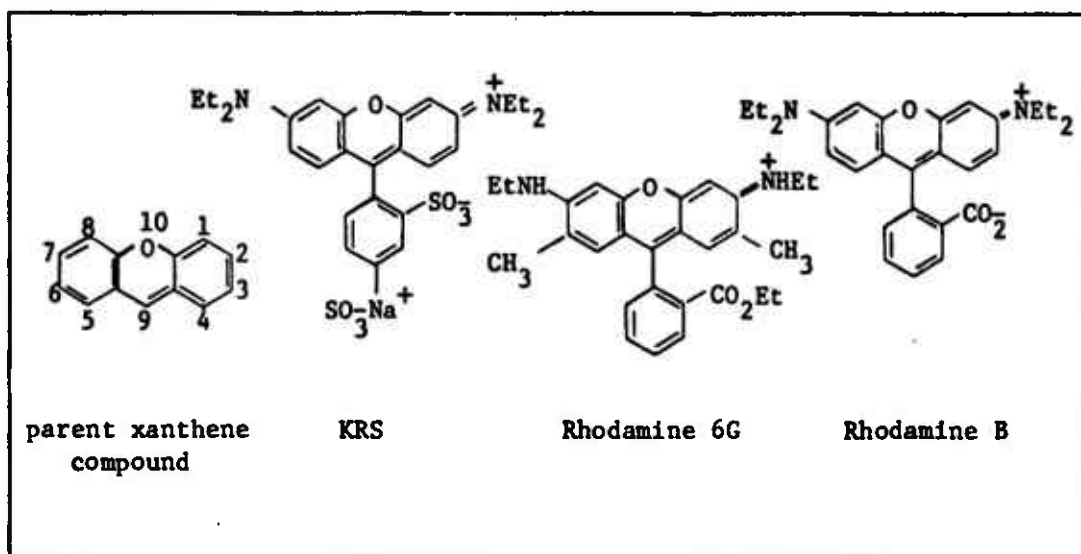
Figure 1

Xanthene Dye Structures

mechanically determine approximate energy level eigenvalues for elec-
tron orbitals (Refs 31:18, 40:31). The energy level diagram of a
typical dye molecule is shown in Figure 2. Aa the conjugated bonds
become longer in the larger molecules, the separation between energy
levela becomea smaller both in this free electron model and experi-
mentally. Therefore the molecules with longer delocalized π bonds
will abaorb at lower spectral energies (Ref 9:184, 40:31).

Due to the large size of the dye molecules and their structural
complexity, many closely-spaced vibronic tranaitions, represented aa
the fine lines within the electronic levels, are possible with each
electronic transition. In addition, every vibrational sublevel is
further divided by rotational sublevels (not depicted) which are
extremely broadened due to frequent collisions with solvent molecules

5
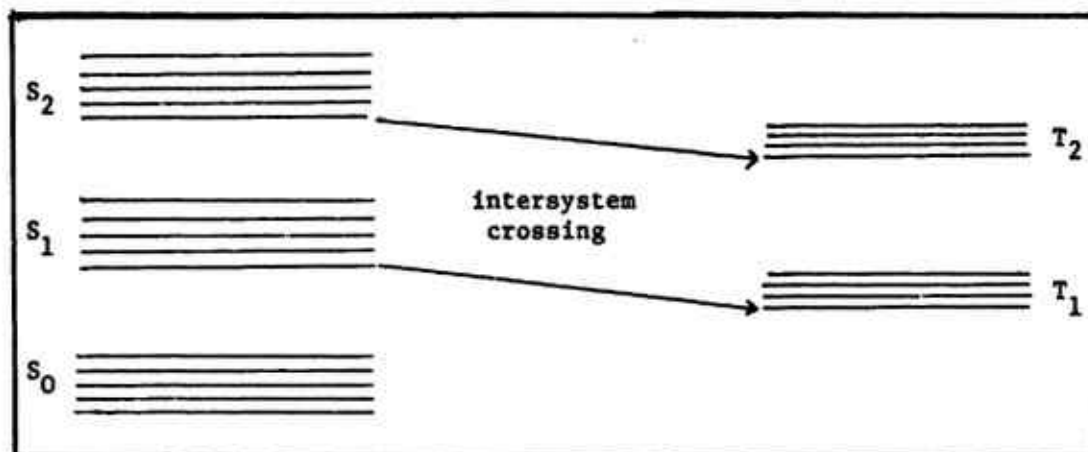
Figure 2

Molecular Energy Levels

(Ref 31:19). The resultant density of these possible transitional
levels provides broad quasi-continuous absorption and fluorescence
bands; the latter band gives KRS a tunability from 589 nm to 642 nm
(Ref 11:270).

The singlet multiplicity states shown on the left in Figure 2
represent the energy eigenstates that a molecule can attain when an
electron transitions to a π^* orbital and has maintained the spin
orientation required in the ground state due to the Pauli exclusion
principle. Once the electron has departed the ground state, it may
change its spin orientation (spin-flip) and occupy one of the triplet
energy levels depicted on the right in Figure 2. Each singlet level
has a corresponding triplet level that is of slightly lower energy.
The triplet levels are primarily populated by nonradiative relaxation
from their corresponding singlet levels as depicted. This process is
known as intersystem crossing. Direct singlet to triplet absorption

6

transitions do occur but at a rate several orders of magnitude slower than intersystem crossing and are therefore negligible. Intersystem crossing can be induced by internal perturbations as well as by external perturbations and the rate varies with the different dyes and as a function of the dye solvent and other parameters (Refs 9, 17, 19, 31:29).

Molecular deexcitation

Once a molecule reaches an excited state it has several paths through which it can return to ground state. These can generally be grouped into radiative and nonradiative transitions.

Radiative Transitions. The radiative transitions are fluorescence and phosphorescence, illustrated in Figure 3. A fluoreacent transition ia one that occurs between states of the same multiplicity; phosphorescent transitions occur between states of different multiplicity and therefore require a spin-flip (Ref 5:308). These terms are used to describe the $S_1 \to S_0$ and $T_1 \to S_0$ transitions respectively in
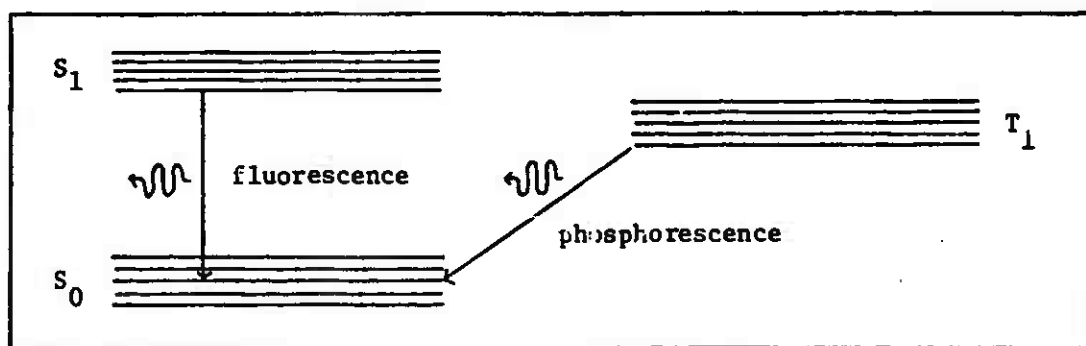
Figure 3

Fluorescence and Phosphorescence

7

the laser dyes. The former transition is usually the lasing transition (Refs 31:29, 37:4726). The rates of these transitions are expressed as the inverse of their lifetimes. The values found in the literature for the fluorescence lifetime τ_F and phosphorescence lifetime τ_P include nonradiative contributions to relaxation:

$$\frac{1}{\tau_F} = \frac{1}{\tau_{F(R)}} + \frac{1}{\tau_{F(NR)}} \qquad (2.1)$$

$$\frac{1}{\tau_P} = \frac{1}{\tau_{P(R)}} + \frac{1}{\tau_{P(NR)}} \qquad (2.2)$$

The subscripts (R) and (NR) refer to radiative and nonradiative lifetimes. The lifetimes τ_F and τ_P therefore give the overall lifetimes of the S_1 and T_1 states due to all relaxation processes (31:30). Fluorescence lifetimes are generally on the order of nanoseconds, while phosphorescence lifetimes usually vary from microseconds to seconds (Refs 31:30, 35:651). For a given compound, however, these values can change as the associated nonradiative relaxation rates are altered by external parameters.

Nonradiative Transitions. In addition to radiative relaxation, excited molecules can relax by several nonradiative processes: by thermal equilibration within the vibronic levels of an electronic state, by internal conversion back to the S_0 level, or by intersystem crossing. When an electronic level becomes significantly populated, thermalization establishes a dynamic equilibrium that results in a Boltzmann distribution among the continum of vibrational and rotational states (Ref 35:650). These distributions are achieved in both the excited and ground state electronic levels and occur on a picosecond time scale (Ref 40:32).

8

Internal conversion takes place between electronic levels of the same multiplicity. Little is actually understood about the phenomena although rates for $S_2 \rightarrow S_1$ and $S_1 \rightarrow S_0$ internal conversion have been experimentally determined for various dyes. $S_2 \rightarrow S_1$ conversion is usually extremely fast, taking place in less than 10^{-11} sec. (Refs 29:962, 31:29). This is the dominant mechanism in depopulation of S_2 and higher-level states. Internal conversion between S_1 and S_0 competes with lasing. This rate has been found to range over several orders of magnitude (Ref 31:29). Figure 4 compares these relaxation processes and gives rates and lifetimes representative of xanthene dyes.

Several nonradiative processes are functions of the solvent and other solute molecules. These environmental effects include fluorescence quenching by charge transfer interactions and aggregation of dye molecules. Aggregation does not occur in organic solvents such as ethanol (Ref 31:159) and charge transfer interactions do not become a factor until the dye concentration exceeds 10^{-3} M (Ref 13:3892) so that neither will be applicable to this analysis.

Quantum Efficiency of Fluorescence. At this point it is worthwhile to define the quantum efficiency of fluorescence Φ. This is a measure of the probability that a dye molecule will emit a photon in fluorescence upon absorption of a photon. This can be expressed as the ratio of radiative and nonradiative transition lifetimes (Ref 31:30):

$$\Phi = \frac{\tau_F}{\tau_{F(R)}} \quad \text{or} \quad \tau_F = \Phi \tau_{F(R)} \tag{2.3}$$

Using the relaxation routes discussed, the formula for Φ would be
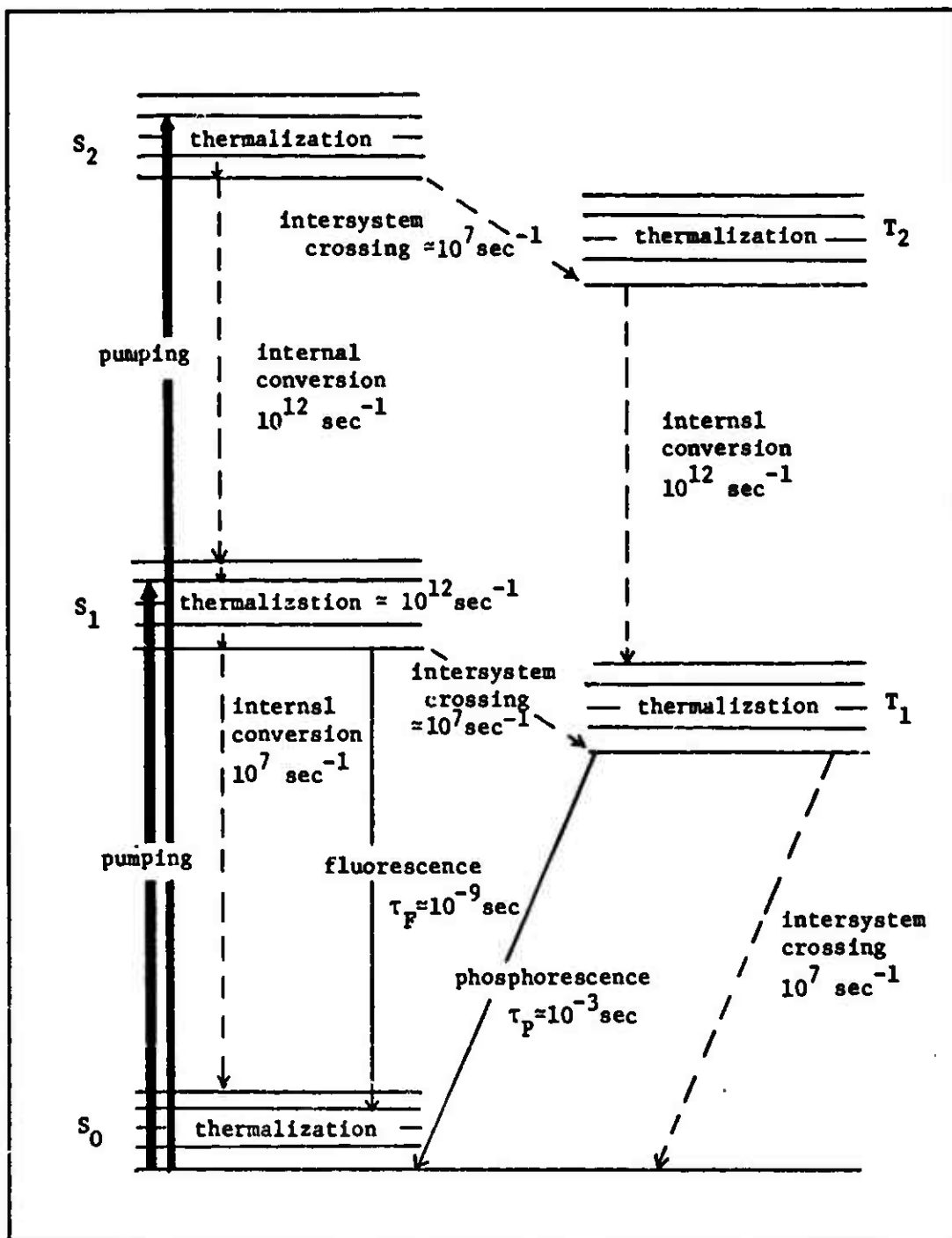
Figure 4

Relaxation Mechanisms

$$\Phi = \frac{\dfrac{1}{\tau_{F(R)}}}{\dfrac{1}{\tau_{F(R)}} + k_{S_1 T_1} + k_{S_1 S_0}} \tag{2.4}$$

where

$k_{S_1 T_1} = S_1 \rightarrow T_1$ intersystem crossing rate

$k_{S_1 S_0} = S_1 \rightarrow S_0$ internal conversion rate

The quantity in the denominator is simply the inverse of the fluorescence lifetime τ_F as previously defined.

Competitive Absorption Processes

Two additional absorption mechanisms have been observed in dye lasers that detract from the lasing efficiency. These are categorized as excited singlet state absorption (ESSA) and triplet absorption. ESSA occurs when S_1 molecules absorb the pump or lasing photons and transition to higher singlet states. They then relax back to the S_1 level primarily by internal conversion (Figure 5). The photons that were absorbed are lost to the lasing process, although the fast relaxation time of internal conversion maintains the population of the S_1 level basically undisturbed. ESSA has been shown to be a significant consideration in most dyes, to the point of quenching the lasing under certain conditions (Refs 29, 30, 42).

Triplet absorption is depicted in Figure 6. This is essentially the same as ESSA but with the absorptions taking place in the triplet manifold. This will only be a factor when lasing parameters allow the T_1 population to build up significantly, such as during long-pulse

11

$h\nu_L$ = energy of lasing transition photon

$h\nu_{\text{p}}$ = energy of pump photon
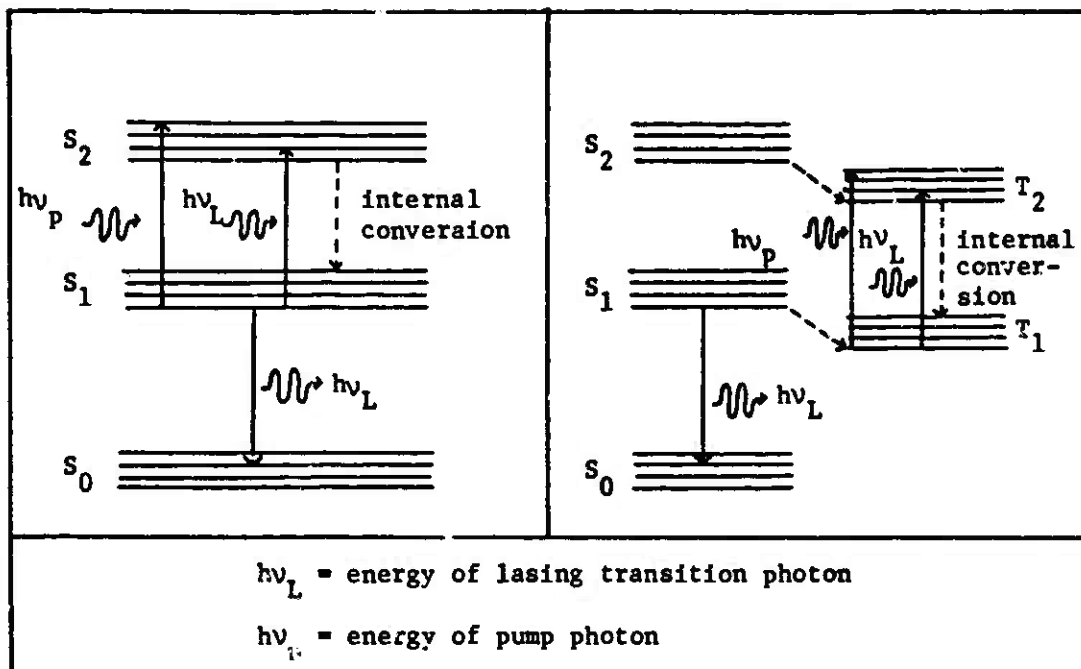
Figure 5   Figure 6

Excited Singlet State Absorption   Triplet Absorption

pumping and CW operation. In these cases, triplet absorption has

also demonstrated the capability to quench lasing (Refs 17, 19).

Quenching

The T_1 population can be controlled with triplet quenching. This

mechanism promotes nonradiative relaxation of the T_1 level to ground

state S_0, increasing the $T_1 \rightarrow S_0$ intersystem crossing rate and therefore

decreasing τ_p. Many triplet quenchers such as molecular oxygen (O_2)

also quench the S_1 level. In many situations the triplet quenching

by O_2 more than offsets its singlet quenching effects, but other com-

pounds have been found that selectively quench the triplet manifold

without the detrimental singlet state quenching. Cyclooctatetraene

has been demonstrated to be an efficient triplet quencher for Rhodamine

6G (Ref 31:59). The rate of quenching is usually expreaaed per unit con-
centration of the quenching agent by the constants k_{QT} and k_{QS} $(M^{-1}sec^{-1})$.

Degradation Effects

The dyes that lase in the long-wavelength range from about 550 nm
into the infrared region are characterized by long conjugated chains
that are particularly susceptible to photodecomposition from the pumping
aource. Most of the xanthene dyes have demonstrated definite photode-
composition which becomes a particularly serious problem under flashlamp
excitation (Refs 8, 15, 16, 25, 33, 34). The precise nature of the
reaction products of KRS have not yet been identified, and no specific
mechanism has been shown to be the cause of the associated laser output
deter:oration (Ref 33). Two likely mechanisms responsible for the loas
of output power as decomposition increases are absorption of the pump
energy and absorption of fluorescence by the reaction products (Refs 12,
18). A third possibility suggested by the latest results of a atudy in
progress (Ref 33) is that the photodegrsdation effectively increases
intersystem crossing to the triplet manifold.

The absorption coefficient α gives the amount of absorption at s
particular wavelength that will occur per centimeter traveled by the
photon beam in a specific medium. If the reaction products were
absorbing lasing photons the absorption coefficient of the dye at the
lasing wavelength would progressively increase as the dye deteriorated.
The lasing efficiency would in turn decrease as more lasing photons
were lost through absorption while oscillating in the cavity.

If the pump photons were being absorbed by the reaction products
the pump efficiency η would decrease. The pump efficiency is defined

13

here as follows:

$$\eta = \frac{\text{theoretical threshold pump power}}{\text{actual pump power required to reach threshold}} \qquad (2.5)$$

The threshold pump power is the power required from the pump to overcome cavity losses and initiate lasing. Pump efficiency considers losses due to pump absorption by impurities in the medium, in addition to losses due to broad-spectrum pumping in which some of the pump photons cannot be absorbed due to improper wavelengths and other losses that prevent the total energy expended by the pump from being absorbed by the dye. A decrease in η would cause a corresponding increase in the actual threshold pump power.

Pulsed Dye Lasers

A simplified schematic for the dye lasing mechanism is shown in Figure 7. The E_1 level population is commonly considered negligible due to thermalization in the ground state electronic level. The thermalization rate is approximately 10^{12}sec^{-1}; the rapidity of this
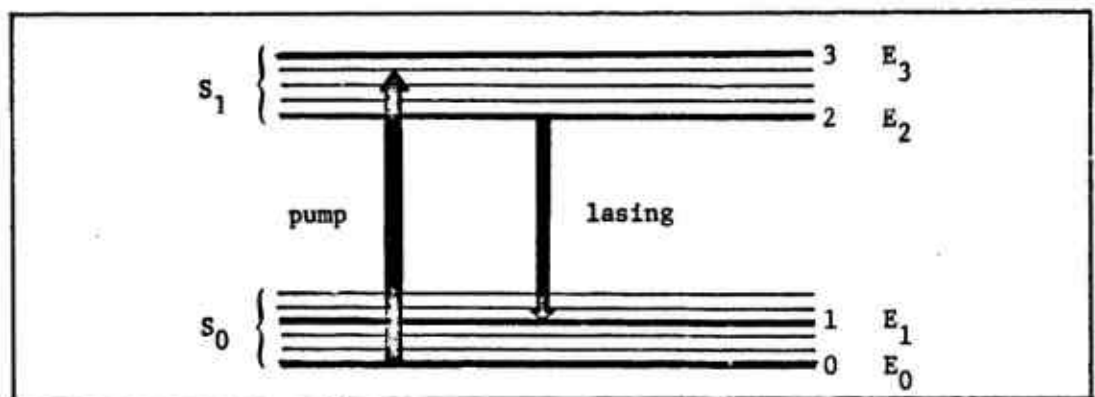
Figure 7

Four-Level Laser Schematic

14

relaxation is due to an ethanol-dye collisional cross-section on the order of $10^{-14} cm^2$. The lasing transition places the molecule into a state that is unpopulated and the molecule then relaxes to the ground level immediately so that a population inversion is effectively established whenever any molecules are in the S_1 level. This is a distinct advantage over systems in which the lasing transition ends in a significantly populated level, and allows lasing to commence with very low threshold pump powers (Ref 41:155). This feature, combined with quantum fluorescence efficiencies greater than 0.7 for the xanthene dyes, gives flashlamp-pumped xanthene dye lasers efficiencies generally from 0.1 to 1 percent; a CW laser pumped by another argon-ion laser has produced light-to-light efficiencies as high as 30 percent (Ref 21:3786).

The population at level 2 can transition to any of the many vibrational-rotational levels within the S_0 state. The broad fluorescence spectrum provides the capability to selectively lase over a wide range of frequencies. One of the most common methods of tuning dye lasers consists of replacing one of the cavity mirrors with a diffraction grating that can be rotated to reflect only the desired wavelength back through the cavity and preclude the remaining wavelengths from oscillating. The singlet-state absorption and fluorescence spectra of Rhodamine 6G in ethanol are reproduced in Figure 8 (Ref 43:188). These spectra are fairly representative of organic dyes. Since the peak of the emission spectrum is at a longer wavelength than the peak of the absorption spectrum, dye lasers can be tuned to lase in a strong emission region away from strong competitive absorption. The separation between the peaks of the absorption and fluorescence spectra is known

15

Singlet-state absorption and fluorescence spectra of rhodamine
6G obtained from measurements with a 10^{-4} molar ethanol solution of the dye.
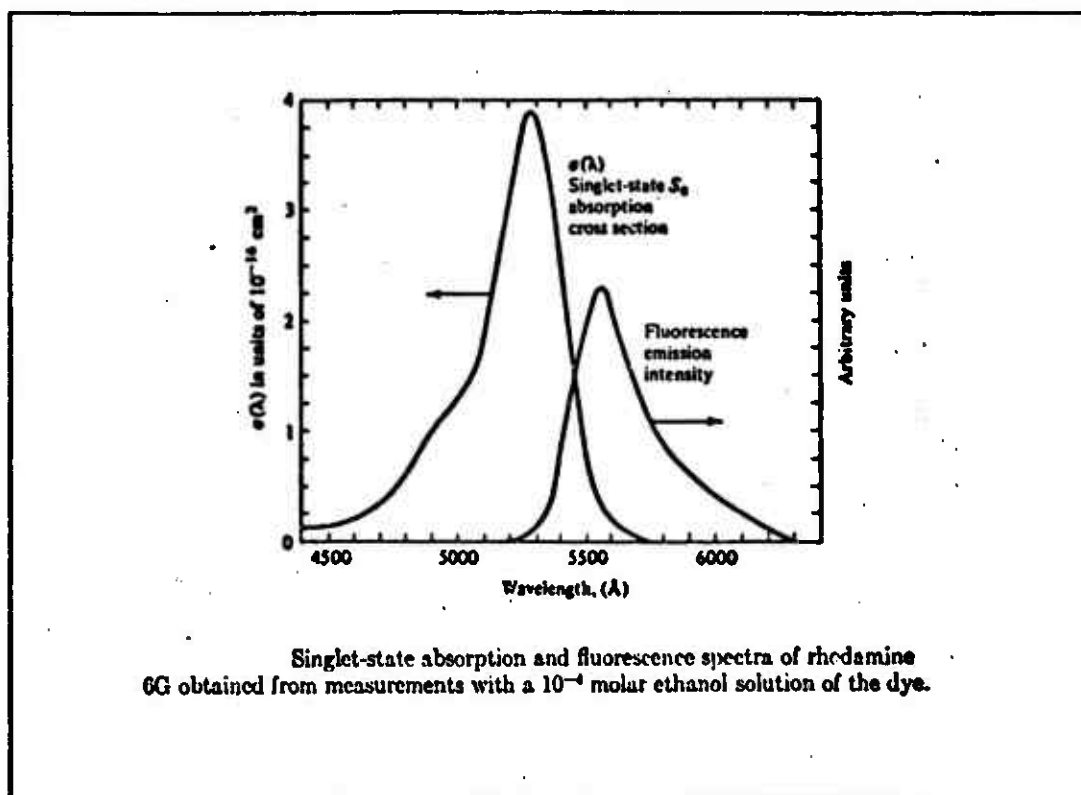
Figure 8

Absorption and Fluorescence Spectra

aa the Stokes Shift. The overlap of the spectra determines the high-
frequency limit of lasing. Some amount of self-absorption will usually
be present at the lasing wavelength and will affect the values of τ_F
and Φ observed (Ref 13).

16

III. Rate Equation Analysis

The absorption, emission, and relaxation processes that were
presented in the preceeding section are illustrated in Figure 9 for
the first two singlet and triplet levels of an organic dye. The dia-
gram demonstrates the interdependence of the various molecular energy
level populations during lasing. The derivation of rate equations for
this system provides a standard method of analysis that considers in
detail the transient and dynamical behavior of the energy level and
cavity photon populations. The literature has examples of many rate
equation analyses of dye lasers that are essentially the same in con-
cept yet use different mathematical techniques to describe lasing
(Refs 1-4, 17, 21, 27, 37, 38). The essential mathematics involved in
the development of the rate equations presented in this section parallel
the approach presented by Siegman (Ref 36:411-431). The equations
necessarily incorporate more concepts than those considered in the
basic model used in this reference. These additional factors were
handled with methods consistent with the literature, if available, or
in the manner judged most suitable by the author. The results are
intended for application to xanthene dye laser systems and therefore
assumptions applicable only to specific dyes such as KRS are withheld
in this section; assumptions limited to xanthene dyes are used only
when great simplification results.

Dye Laser Model

The mechanisms summarized in Figure 9 appear to have the most
probable impact on dye laser performance; the relative importance of

17
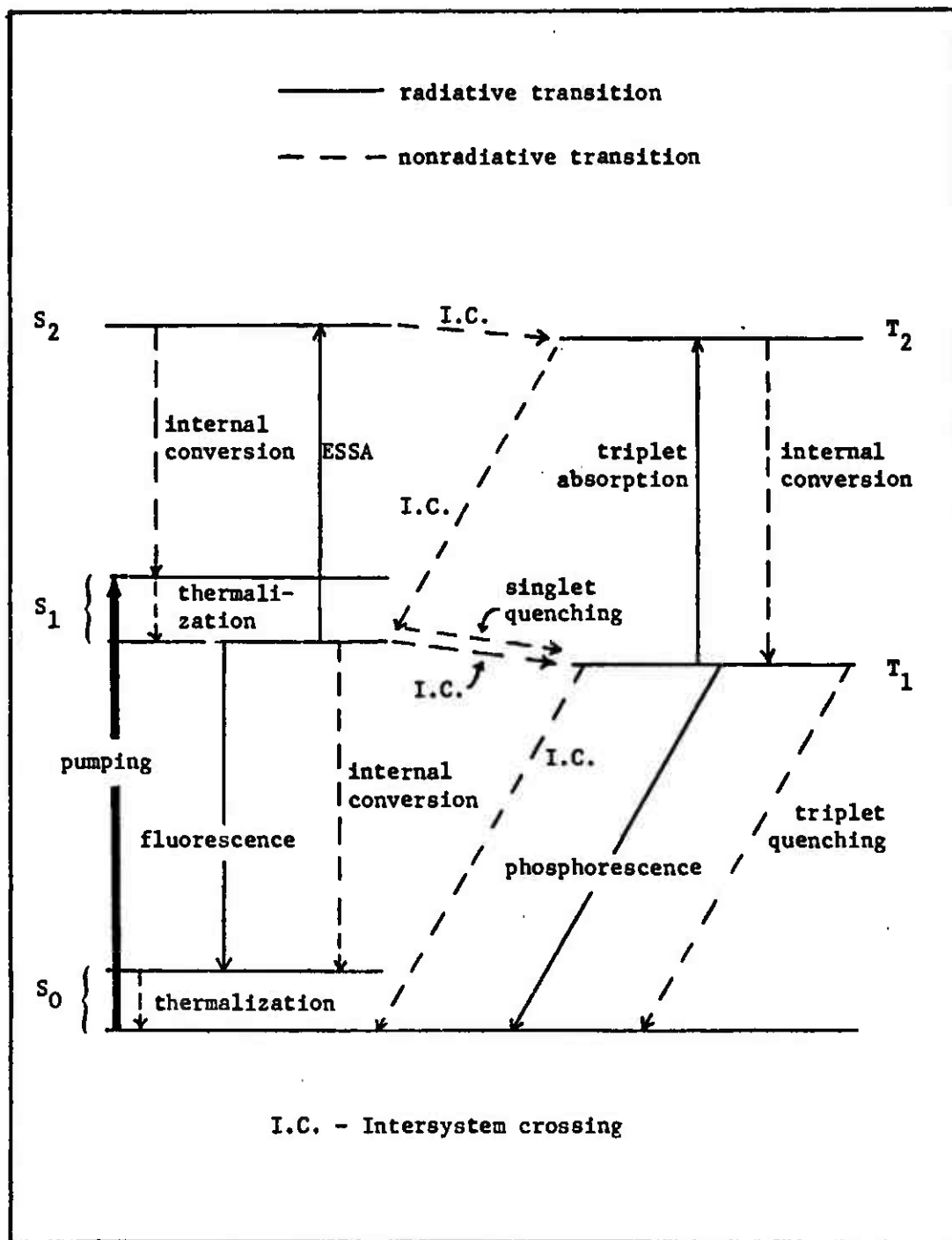
Figure 9

Excitation and Relaxation Paths in Laser Dyes

each depends on the chemistry of the particular dye that is being examined. For the great majority of dyes the upper level internal conversion rates are extremely fast, on the order of 10^{12} aec^{-1}, ao the S_2 and T_2 populations should remain minimal and interactions from these and higher levels will be considered negligible (Ref 29:963). The $T_2 \rightarrow S_1$ intersystem crossing rate would also be negligible in compariaon to the $T_2 \rightarrow T_1$ internal conversion rate. The rate equations are developed around single mode operation of a laser that is homogeneously broadened (Ref 35:650). The cavity photon population (n) is assumed to be spatially uniform (Ref 40:37A). Schlieren effects are not addressed.

To initially focus on the most likely effects of reaction product formation a simplified four-level model that takes into account both excited singlet state absorption and triplet absorption is used (Figure 10). By making the assumption that the S_2, T_2, and upper-level S_1 and S_0 populations are immediately depleted by internal conversion and thermalization and are therefore negligible, these levels may be explicitly left out of the equations. It should be noted that although these populations are not addressed by the rate equations, terms that consider ESSA and triplet absorption of fluorescence photons can be introduced into the cavity photon population equation. By handling the absorption in this manner the absorbed photons are lost to the photon population yet the E_2 and E_3 populations remain unaffected. Several recent publications (Refs 1-4) include the T_2 and upper-level S_1 levels to allow a more detailed examination based on a six-level system (the S_2 level remains deleted). Appendix A presents an equation set based on this six-level model that also includes ESSA. These equations would enable a more

19
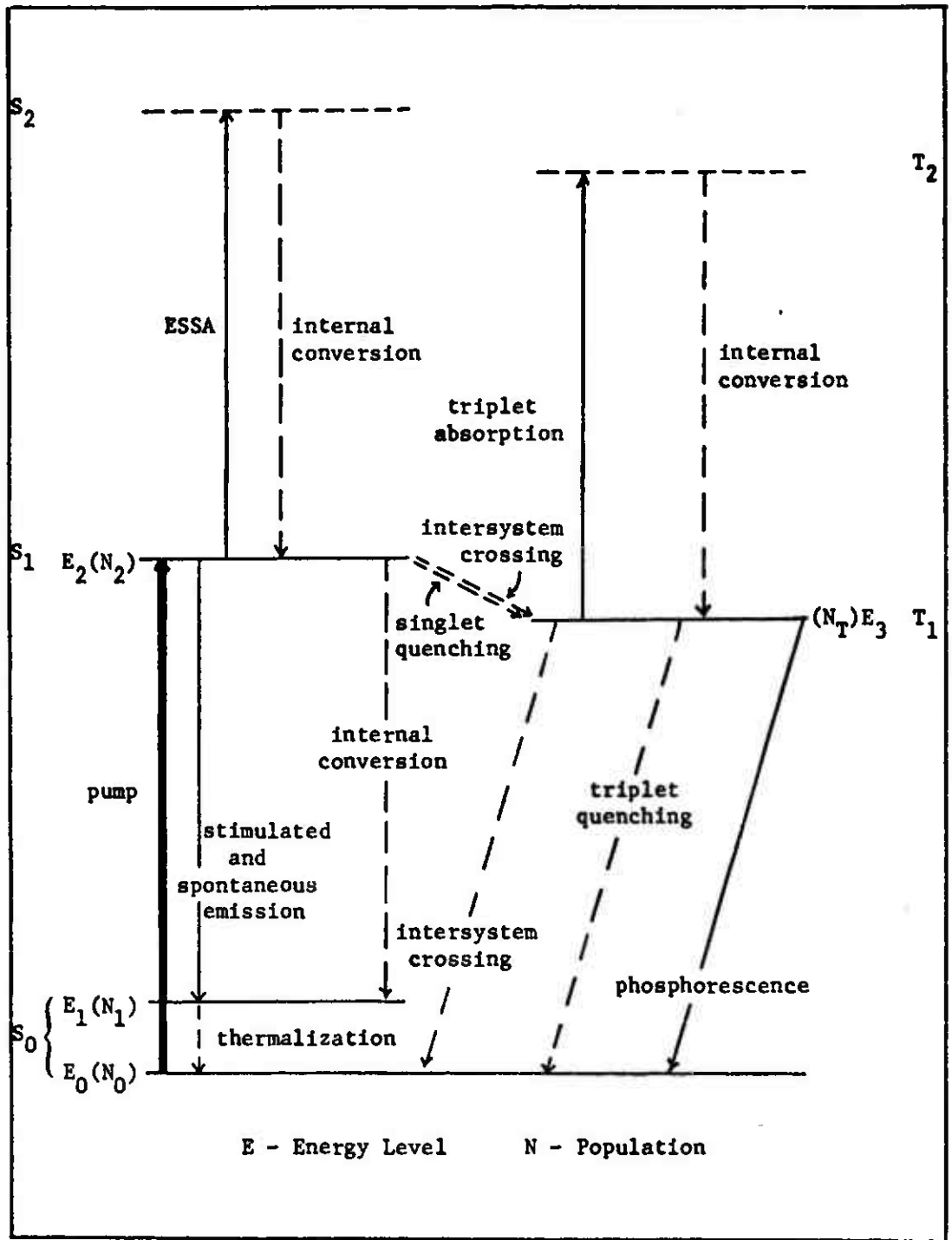
Figure 10

Rate Equation Model

refined analysis, particularly in conjunction with non-stationary
computer solutions.

Rate Equations

The rate equation for the cavity photon population is

$$\frac{dn}{dt} = \frac{N_2 n}{\tau_{F(R)}} + \frac{N_2}{\tau_{F(R)}} - \frac{N_2 n}{\delta_S \tau_{F(R)}} - \frac{N_T n}{\delta_T \tau_{F(R)}} - \frac{n}{\tau_C} \qquad (3.1)$$

where

N_2 = E_2 energy level population density

N_T = E_3 energy level population density

$\tau_{F(R)}$ = radiative fluorescence lifetime

τ_C = cavity photon lifetime

δ_T = ratio of the $S_0 \rightarrow S_1$ extinction coefficient to the $T_1 \rightarrow T_2$ extinction coefficient at the lasing wavelength

δ_S = ratio of the $S_0 \rightarrow S_1$ extinction coefficient to the $S_1 \rightarrow S_2$ extinction coefficient at the lasing wavelength

The first two terms on the right in Eq (3.1) account for stimulated and
spontaneous emissions from level 2; the spontaneous emission occurs at
the same rate as stimulated emission when the photon population is set
equal to 1 (Ref 36:416). The third and fourth terms account for ESSA
and triplet absorption losses respectively. These terms were adapted
from a triplet absorption expression in Keller's presentation (Ref
17:411). The ratios $N_2 n/\tau_{F(R)}$ and $N_T n/\tau_{F(R)}$ give absorption rates
assuming the Einstein B coefficients for the $S_1 \rightarrow S_2$ and $T_1 \rightarrow T_2$ transi-
tions are equal to the Einstein B coefficient for the $S_0 \rightarrow S_1$ transition.
The δ factors in the denominators adjust the rates to account for the

21

actual differences in the B coefficients. The final term reflects losses associated with cavity parameters such as mirror transmission and ground state absorption by the laser medium at the lasing wavelength. The absorption coefficient of the dye solution at the lasing wavelength will increase with dye degradation if the reaction products absorb fluorescence photons; this increase will decrease τ_C. The first two terms in Eq (3.1) can be combined:

$$\frac{dn}{dt} = \frac{N_2}{\tau_{F(R)}}(n+1) - \frac{N_2 n}{\delta_S \tau_{F(R)}} - \frac{N_T n}{\delta_T \tau_{F(R)}} - \frac{n}{\tau_C} \tag{3.2}$$

The rate equation for N_2 is

$$\frac{dN_2}{dt} = W(t)\eta - \frac{N_2}{\tau_{F(R)}}(n+1) - N_2(k_{S_1 T_1} + k_{S_1 S_0} + k_{QS} Q_S) \tag{3.3}$$

where

$W(t)$ = pumping function

η = quantum pumping efficiency

$k_{S_1 T_0}$ = $S_1 \rightarrow T_1$ intersystem crossing rate constant

$k_{S_1 S_0}$ = $S_1 \rightarrow S_0$ internal conversion rate constant

k_{QS} = singlet quenching rate constant

Q_S = concentration of singlet quencher

The pumping function can be varied to describe the characteristics of the particular method of pumping. Linear and Gaussian models have commonly been used for flashlamp pumping (Refs 4, 17, 21, 29, 37).

The remaining rate equation is for N_T:

$$\frac{dN_T}{dt} = N_2(k_{S_1T_1} + k_{QS}Q_S) - \frac{N_T}{\tau_{P(R)}} - N_T(k_{T_1S_0} + k_{QT}Q_T) \qquad (3.4)$$

where

$\tau_{P(R)}$ = radiative phosphorescence lifetime

$k_{T_1S_0}$ = $T_1 \rightarrow S_0$ intersystem crosaing rate constant

k_{QT} = triplet quenching rate constant

Q_T = concentration of triplet quencher

Here it is assumed that singlet quenching increases intersystem crossing to the triplet manifold (Ref 31:58), augmenting the N_T population; the possibility also exists that it returns the moleculea directly to the ground state (Ref 17:412). Pumping directly to the triplet manifold is neglected.

A rste equation for N_0 is not required as this population's only interaction on lasing in the model has been represented by $W(t)$. As long as the N_0 molecules are replenished during actual lasing under pulsed excitation, a generalized $W(t)$ function can successfully be used to describe the pulse of pump photons generated and N_2 will follow the pumping rste in both the actual laser and the model. If the N_0 molecules are significantly depleted during the lasing due to entrspment in the triplet manifold then the reduced pump photon absorption by N_0 will not be reflected adequately by these equations and a closed-population system of rate equations that include N_0 should be used (aee Appendix A). This requirement is not anticipated for the xanthene dyes due to their high fluorescence efficiencies which indicate small triplet build-up rstes. Triplet quenching and short flashlamp pulae duration alao minimize triplet populations.

23

The complete set of rate equations is then

$$\frac{dn}{dt} = \frac{N_2}{\tau_{F(R)}}(n+1) - \frac{N_2 n}{\delta_S \tau_{F(R)}} - \frac{N_T n}{\delta_T \tau_{F(R)}} - \frac{n}{\tau_C} \qquad (3.2)$$

$$\frac{dN_2}{dt} = W(t)\eta - \frac{N_2}{\tau_{F(R)}}(n+1) - N_2(k_{S_1 T_1} + k_{S_1 S_0} + k_{QS}Q_S) \qquad (3.3)$$

$$\frac{dN_T}{dt} = N_2(k_{S_1 T_1} + k_{QS}Q_S) - \frac{N_T}{\tau_{P(R)}} - N_T(k_{T_1 S_0} + k_{QT}Q_T) \qquad (3.4)$$

Steady-State Solutions

In most cases of interest a steady-state approximation to the rate equations simplifies their application and yields results comparable to the more demanding numerical methods of solution (Ref 17). This adiabatic approximation has been shown to favorably compare with numerical solutions of the rate equations for both CW operation and flashlamp pumping with pulses as short as one nanosecond (Ref 29:963). The flashlamp pulse duration was 500 nanoseconds in Rabins' experiment; the steady-state approximation should therefore yield useful results. The resulting equations are

$$\frac{N_2}{\tau_{F(R)}}(n+1) = \frac{N_2 n}{\delta_S \tau_{F(R)}} + \frac{N_T n}{\delta_T \tau_{F(R)}} + \frac{n}{\tau_C} \qquad (3.5)$$

$$W(t)\eta = \frac{N_2}{\tau_{F(R)}}(n+1) + N_2(k_{S_1 T_1} + k_{S_1 S_0} + k_{QS}Q_S) \qquad (3.6)$$

$$N_2(k_{S_1 T_1} + k_{QS}Q_S) = \frac{N_T}{\tau_{P(R)}} + N_T(k_{T_1 S_0} + k_{QT}Q_T) \qquad (3.7)$$

Equations (3.6) and (3.7) can be simplified by grouping their respective radiationless rate constants into one rate constant:

$$k_2 = k_{S_1 T_1} + k_{S_1 S_0} + k_{QS} Q_S \qquad (3.8)$$

$$k_{ST} = k_{S_1 T_1} + k_{QS} Q_S \qquad (3.9)$$

$$k_T = k_{T_1 S_0} + k_{QT} Q_T \qquad (3.10)$$

Equations (3.6) and (3.7) then become

$$W(t)\eta = \frac{N_2}{\tau_{F(R)}} - (n+1) + N_2 k_2 \qquad (3.11)$$

$$N_2 k_{ST} = \frac{N_T}{\tau_{P(R)}} + N_T k_T \qquad (3.12)$$

Recalling Eqs (2.1) and (2.2), Eqs (3.11) and (3.12) can alternately be expressed as

$$W(t)\eta = \frac{N_2 n}{\tau_{F(R)}} + N_2 \left(\frac{1}{\tau_F}\right) \qquad (3.13)$$

$$N_2 k_{ST} = N_T \left(\frac{1}{\tau_P}\right) \qquad (3.14)$$

Replacing τ_F in Eq (3.13) by $\phi \tau_{F(R)}$, we can write

$$W(t)\eta = \frac{N_2}{\tau_{F(R)}} \left(n + \frac{1}{\phi}\right) \qquad (3.15)$$

25

Solving Eq (3.5) for n, we get

$$n = \frac{N_2}{N_2\left[\dfrac{1}{\delta_S} - 1\right] + \dfrac{N_T}{\delta_T} + \dfrac{\tau_{F(R)}}{\tau_C}} \qquad (3.16)$$

The above-threshold condition occurs when the denominator approaches zero; this gives the above-threshold population for N_2 ($N_{2,TH}$):

$$N_{2,TH} = \left[\frac{N_T}{\delta_T} + \frac{\tau_{F(R)}}{\tau_C}\right]\left[\frac{\delta_S}{\delta_S - 1}\right] \qquad (3.17)$$

N_2 saturates at this value so that above threshold $N_2 = N_{2,TH}$ (Ref 36: 424).

Solving Eq (3.12) for N_T and substituting this value into Eq (3.17) we obtain

$$N_{2,TH} = \frac{\tau_{F(R)}}{\tau_C}\left[\frac{\delta_S\delta_T\ (k_T\tau_{P(R)}+1)}{\delta_S\delta_T(k_T\tau_{P(R)}+1) - \delta_T(k_T\tau_{P(R)}+1) - k_{ST}\delta_S\tau_{P(R)}}\right] \qquad (3.18)$$

Assuming $k_T\tau_{P(R)} \gg 1$, Eq (3.18) can be simplified:

$$N_{2,TH} = \frac{\tau_{F(R)}}{\tau_C}\left[\frac{\delta_S\delta_T k_T}{\delta_S\delta_T k_T - \delta_T k_T - k_{ST}\delta_S}\right] \qquad (3.19)$$

Above threshold, $n \gg 1$ so that Eq (3.15) can be approximated by

$$W(t)\eta \simeq \frac{N_{2,TH}}{\tau_{F(R)}}(n) \quad \text{or} \quad n \simeq W(t)\eta\frac{\tau_{F(R)}}{N_{2,TH}} \qquad (3.20)$$

The output power of the laser (P_{laser}) can now be expressed as

26

$$P_{laser} = \frac{nh\nu_L}{\tau_M} \tag{3.21}$$

where

h = Planck's conatant (6.626×10^{-34} joule-sec)

ν_L = frequency of the lssing photon

τ_M = cavity photon lifetime due to mirror transmission only

The threshold pumping rate $W_{P,TH}$ is defined by the follcwing equation:

$$W_{P,TH} = \frac{N_{2,TH}}{\tau_F \eta} \tag{3.22}$$

This equation is based on one developed by Siegman (Ref 36:424) with the addition, for the present analysis, of η to account for possible loaa in pump efficiency due to reaction product absorption. Aa $N_{2,TH}$ ia an implicit function of α due to its dependence on τ_C, $W_{P,TH}$ will increaae with either pump or lasing absorption by the reaction products.

IV. Analysis of the Kiton Red S Laser

The rate equations presented in Section III now provide a means to examine KRS under flashlamp pumping and to attempt explanation of the multiplier effect observed by Rabins et al. (Ref 25). To the maximum extent possible this analysis will employ data directly from their experiments to reproduce their conditions and then try to obtain similar results analytically.

Calculation of Pulse Energy

Eq (3.21) expresses the power output of a laser as a function of the cavity photon population:

$$P_{laser} = \frac{nh\nu_L}{\tau_M} \tag{3.21}$$

The assumption that $k_T \tau_{P(R)} \gg 1$ is valid for $\tau_{P(R)} > 10^{-4}$ sec and $k_{T_1 S_0} \geq 10^6$ sec^{-1}. Both of these conditions are very probable (Ref 32) although no specific data for $k_{T_1 S_0}$ and $\tau_{P(R)}$ were discovered in the literature for KRS or the other xanthene dyes. Allowing this assumption, we can combine Eqs (3.19) and (3.20) to arrive at the following expression for P_{laser}:

$$P_{laser} = \frac{h\nu_L W(t)\eta\tau_C}{\tau_M} \left[\frac{\delta_S \delta_T k_T - \delta_T k_T - k_{ST}\delta_S}{\delta_S \delta_T k_T} \right] \tag{4.1}$$

The expressions for τ_C and τ_M are dependent upon the laser cavity geometry and are derived in Appendix B:

$$\tau_C = \left\{ \frac{cL}{\ell + L(n_D - 1)} \left[\alpha + \frac{1}{2L} \ln\left(\frac{1}{R_1 R_2}\right) \right] \right\}^{-1} \qquad (4.2)$$

$$\tau_M = \left[\frac{c}{2\ell + 2L(n_D - 1)} \ln\left(\frac{1}{R_1}\right) \right]^{-1} \qquad (4.3)$$

where

c = speed of light in vacuum

L = length of dye medium traversed by a photon during a single pass through the laser cavity

ℓ = distance between mirrors in the laser cavity

n_D = index of refraction of the dye solution

α = absorption coefficient of the dye solution at the lasing wavelength

R_1 = reflectivity of the frontal cavity mirror

R_2 = reflectivity of the rear cavity mirror

As the dye degrades, fewer dye molecules are available to absorb the pump photons and lase. The term Π is introduced to account for this reduction in dye concentration and its resultant decrease in output power. The derivation of values for Π is given in Appendix C. Substituting Eq (4.3) into (4.1) and including Π in the equation we arrive at

$$P_{laser} = \frac{\Pi h \nu_L c W(t) \eta \tau_C}{2\ell + 2L(n_D - 1)} \ln\left(\frac{1}{R_1}\right) \left[\frac{\delta_S \delta_T k_T - \delta_T k_T - k_{ST} \delta_S}{\delta_S \delta_T k_T} \right] \qquad (4.4)$$

Eq (4.4) gives the output power of the laser in terms of $W(t)$. The function used for $W(t)$ in this analysis is the Gaussian distribution pulse approximation (Refs 17, 37, 38):

$$W(t) = W_{max} \exp \left\{ - \left[\left(\frac{t}{T_1} \right) (\ln 2)^{1/2} \right]^2 \right\} \qquad (4.5)$$

T_1 is the half-width at half-height of the pumping pulse. This pulse peaks at the value W_{max} (photons/sec) at time $t=0$.

To calculate the energy in a shot the pulse was divided into 1 nano-second units and the output power determined for each increment. The resultant power curve was integrated over the duration of the pulse by computer using a trapezoidal area approximation. The computer program used to calculate the pulse energy for different shots as the variables changed is listed in Appendix D.

Experimental Data

The experiment conducted by Rabins consisted of six photolysis trials. In the first three trials the amount of dye degradation that occurred during successive flashlamp pulses and the related pulse energy were determined. The dye solution in Trial 1 was purged with argon to remove the oxygen from the solution. Trials 2 and 3 had 1.0×10^{-3} M and 2.1×10^{-3} M of oxygen in solution respectively (Ref 25:45). These measurements were repeated in Trials 4 through 6 with the addition of a filter to eliminate high-energy regions of the pump spectrum. The dye solution in Trial 4 was purged with argon; Trials 5 and 6 had 2.1×10^{-3} M oxygen in solution. The degradation and output energy data used in the computer analysis were taken from the graphs in Appendix E which give the results of the first three trials (Ref 25:30-35). The dye concentration c_D was determined from the linear fitting on the graph rather than the plotted points to provide ideal data that simplified the interpretation of the theoretical results. For the same reason the data

was recorded to three decimal places. Table I lists the values used for theae trials in the analysis.

Parameter Values

The values used for the independent parameters of the pulse energy are listed in Table II. A distinction is made here between parameters and variables: the parameters are considered constant throughout a trial, while the variables change with shot number. The dependent parameters τ_F, τ_p, and Φ also remain conatant through the trial since they are functions of the independent parametera. The values of τ_F, τ_p, and Φ that were calculated from the independent parameter valuea in Table II are listed in Table III.

Tables II and III illustrate the difficulty encountered in trying to locate consistent values for the KRS parameters. Many of these parametera are difficult to evaluate in the laboratory and most of the data found in the literature was for Rhodamine 6G and Rhodamine B. Fortunately the analysis of pumping and lasing radiation absorption allows considerable latitude in the selection of these values as the independent parameters affect the absolute power output rather than the output difference between shots. This is apparent when we examine the expression for the output power given by Eq (4.4):

$$P_{laser} = \frac{\Pi h \nu_L c W(t) \eta \tau_C}{2\ell + 2L(n_D - 1)} \ln\left(\frac{1}{R_1}\right)\left[\frac{\delta_S \delta_T k_T - \delta_T k_T - k_{ST}\delta_S}{\delta_S \delta_T k_T}\right] \quad (4.4)$$

The variables Π, η, and τ_C are the only factors that reflect changes in pump and lasing absorption; the independent parameters δ_S, δ_T, k_T, and k_{ST} will all remain unaffected. Singlet quenching by a reaction product

31

Table I

Experimental Data

Trial	Shot Number	Dye Concentration c_D (10^{-4} M)	O_2 Concentration (M)	Shot 1 Energy* (mJ)	Laser Half-Life (# Shots)
1	1 500 1000 1500 2000 2500 3000	1.935 1.870 1.805 1.740 1.675 1.610 1.545	0.0	250	550
2	1 500 1000 1500 2000 2500 3000	1.960 1.922 1.884 1.846 1.808 1.770 1.732	1.0×10^{-3}	245	500
3	1 500 1000 1500 2000 2500 3000	2.000 1.964 1.928 1.892 1.856 1.820 1.784	2.1×10^{-3}	215	450

L = 28.0 cm ℓ = 25.0 cm R_1 = 0.99 R_2 = 0.22 n_D = 1.36 (99.8% ethanol @ 20°C)

(Ref 25:16, 18)

* from Figures E-2, E-4, and E-6

Table II

Independent Parameter Values

Parameter	Value Used	Values Reported		Reference
$\tau_{F(R)}$ (sec)	3.1×10^{-9}	----		----
$\tau_{P(R)}$ (sec)	10^{-3}	----		----
$k_{S_1 S_0}$ (sec^{-1})	10^7	$10^7 - 10^8$		
$k_{S_1 T_1}$ (sec^{-1})	2.5×10^7	1.8×10^7 2×10^7 $1.5 - 6.7 \times 10^7$	(1) (1) (3)	19:229 31:58 37:4732
$k_{T_1 S_0}$ (sec^{-1})	10^7	10^7		32
k_{QS} (M^{-1}sec^{-1})	3×10^9	3×10^{10} 2×10^{10}	(1) (4)	31:58 17:415
k_{QT} (M^{-1}sec^{-1})	10^7	10^7 3.3×10^9 2.5×10^9	 (1) (4)	33:2 31:58 17:415
δ_T	10	10	(1) (3) (4)	21 37:4728 17
δ_S	10	----	(5)	----

(1) - Rhodamine 6G
(2) - Rhodamine B
(3) - Xanthene dyes in general
(4) - No specific dye referred to when given
(5) - Based on the following values for ESSA and triplet absorption cross sections for Rhodamine 6G:

$$\sigma_T = 0.35 \times 10^{-16} cm^2 \quad (Ref \ 19:229)$$

$$\sigma_{S_1 \to S_2} = 0.4 - 0.6 \times 10^{-16} cm^2 \quad (Ref \ 29:966)$$

will change k_{ST}, however, so that the values chosen for the associated relaxation rates will have some effect on the magnitude of change between successive shots when analyzing this mechanism. The value for W_{max} was arbitrarily selected for each set of independent parameter values to equate the pulse energy of the first shot calculated by the computer program to the experimental value. A change in output energy due to varying a parameter could be absorbed by increasing or decreasing W_{max} to compensate for the change.

Table III

Dependent Parameter Values

Parameter	Calculated Value	Values Reported		Reference
τ_F (sec)	2.8×10^{-9}	2.8×10^{-9}		9:85
		3.1×10^{-9}		13:3892
		5×10^{-9}	(3)	37:4728
τ_P (sec)	1.0×10^{-7}	10^{-6}	(3)	6:421
		2×10^{-6}	(1)	31:59
		1.4×10^{-7}	(1)*	31:59
Φ	0.90	0.99		13:3890
		0.83±0.02		9:185
		0.9	(3)	37:4728

(1) Rhodamine 6G

(3) Xanthene dyes in general

* with 20% oxygen content in atmosphere above dye

The figure given for k_{QT} from the Battelle Laboratories interim report (Ref 33) in Table II was much lower than would be expected from the previously reported figures also listed. This value may explain the reduction of output power Rabins noted in Trials 2 and 3 (see Table I). If k_{QS} remains on the order of 10^9-10^{10} sec^{-1} oxygen would prove to be more detrimental due to singlet quenching than beneficial due to triplet quenching. The values used in the analysis for k_{QS} and k_{QT} duplicated the initial output energies listed in Table I to within 10 mj while holding W_{max} constant.

Trial Variables

The computer analysis was designed to work with three variables: the solution pump absorption factor Π, the quantum pump efficiency η, and the absorption coefficient α of the dye solution at the lasing wavelength (λ_L).

Pump Absorption Factor Π. The pump absorption factor was designed to compensate for the reduction in the dye concentration as lasing progressed. This variable is also dependent on the amount of the reaction product present if the reaction product absorbs the pump photons. Appendix C tabulates in Tables C-I and C-II the values for Π in both cases and shows how these figures were calculated. Figure 11 presents the graph of the pulse energies computed using Π as the only variable and compares this with the experimental values. This case represents the reduction in output due only to the reduced concentration of the dye. This factor is included in all of the following evaluations, using the appropriate values from Tables C-I and C-II.

Pump Efficiency η'. This term is used to account for the reduced probability of a pump photon being absorbed by a dye molecule as

35

competitive absorption by the reaction products increases. This variable has been isolated from the remaining factors in the total pump efficiency η as defined in Eq (2.5) for the purposes of the analysis. Appendix C explains the derivation of η'. This variable replaces η in the equation developed for the analysis.

Figure 12 is a graph of the concentration of dye versus shot number based on visible spectra (Ref 25:46). This appears contradictory to Figure E-3 which was determined from infrared (IR) spectra. Figure 12 indicates that absorption of pump photons at 552 nm by the dye solution increases initially with shot number. This could be due to the formation of a transient reaction product that absorbs at this wavelength but does not interfere with the absorption at the IR band used to determine the concentration curve in Figure E-3. Due to the uncertainty surrounding reaction product formation and identity several ratios of dye degradation to reaction product formation were formulated. The values for both η' and Π corresponding to these ratios that were used to examine pump absorption are provided in Table C-II. The analytical results based on these values are presented in Figure 13.

Absorption Coefficient α. The variable α changes as the dye degradation alters the absorption capability of the dye solution. Figures 14 and 15 are the absorption spectra of the Trial 1 dye solution before lasing (shot 0) and after 3000 shots (Ref 26:95). A distinct reduction in absorption of the dye around 460 nm is obvious; this peak corresponds to $S_0 \rightarrow S_1$ absorption. If the reaction products were increasing the absorption coefficient for the 625 nm to 635 nm λ_L region, a decrease in I/I_0 for shot 3000 should be indicated within this band. The maximum decrease in I/I_0 that could be consistent with Figures 14 and 15 was
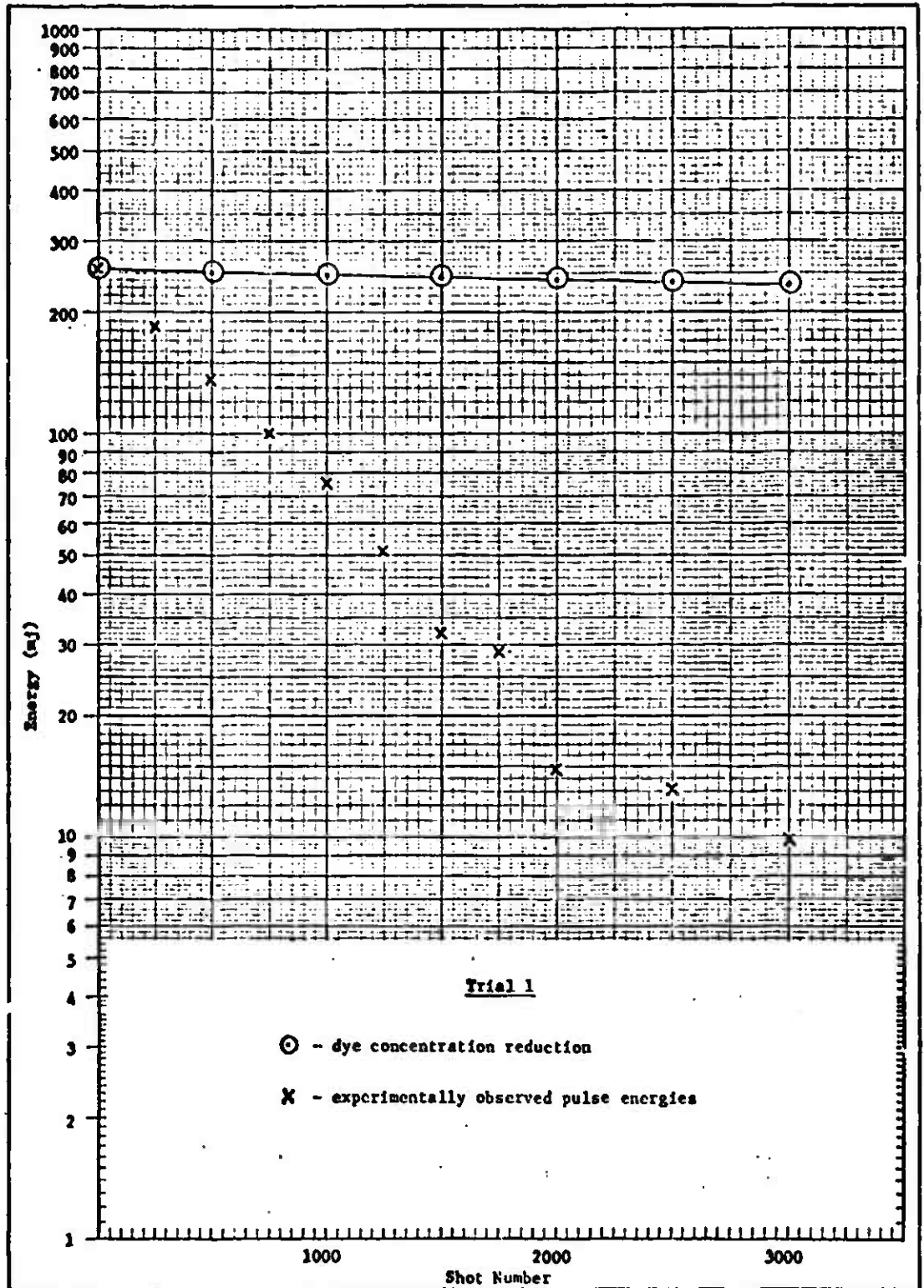
36

Figure 11

Pulse Energies due to Dye Concentration Reduction

37
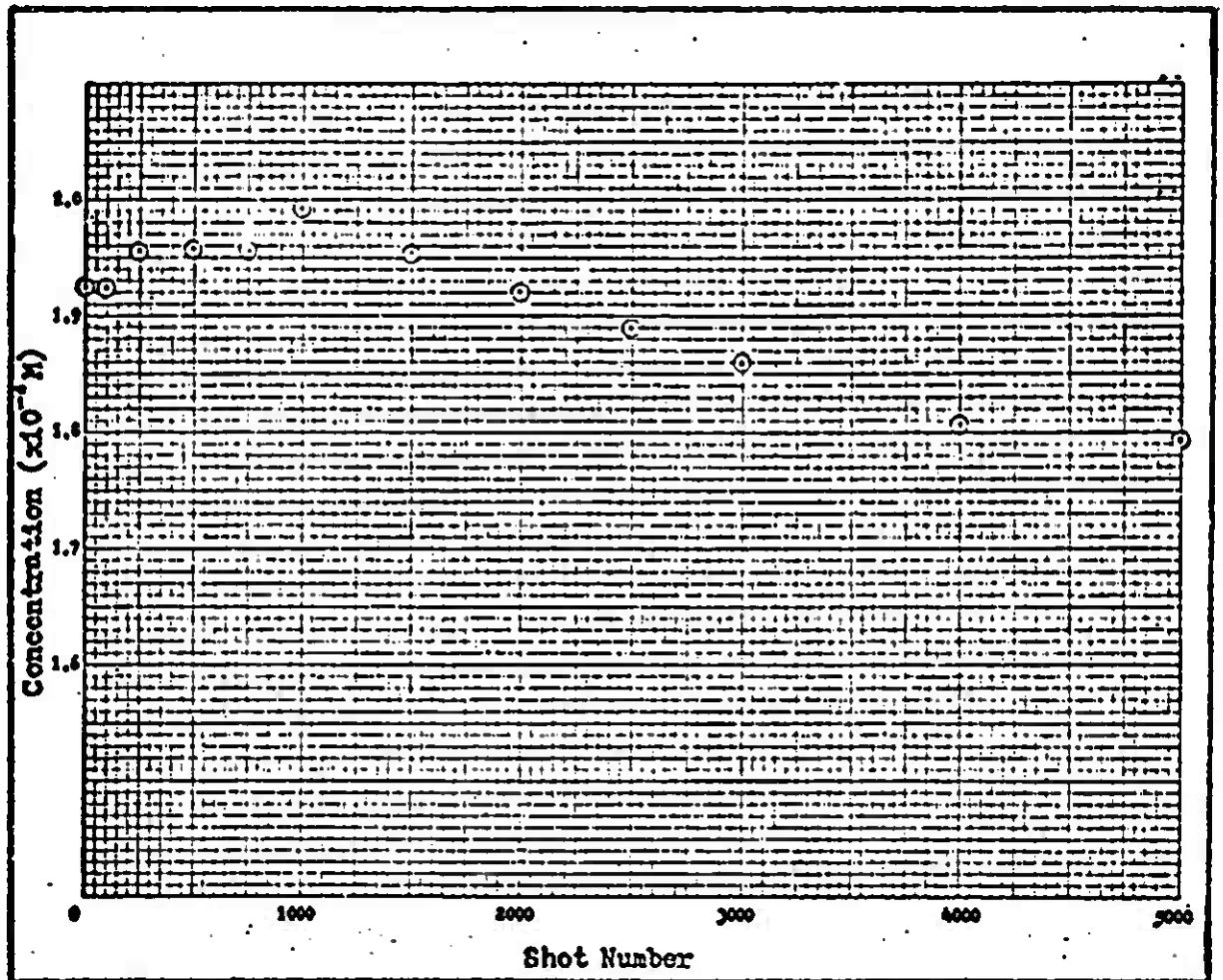
Figure 12

Dye Concentration Versus Shot Number (Visible Spectra)
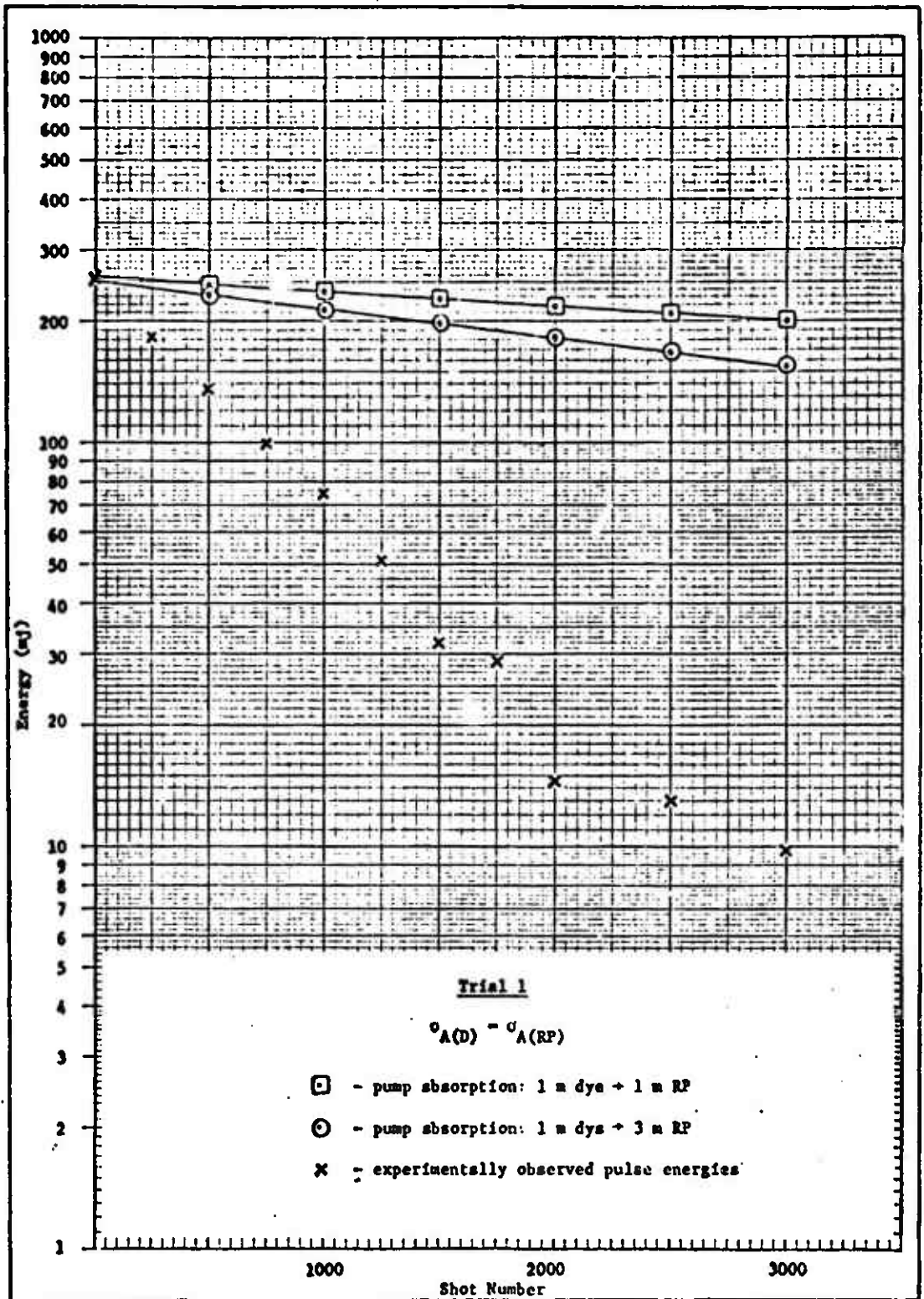
Figure 13

Pulse Energies due to Pump Absorption

39
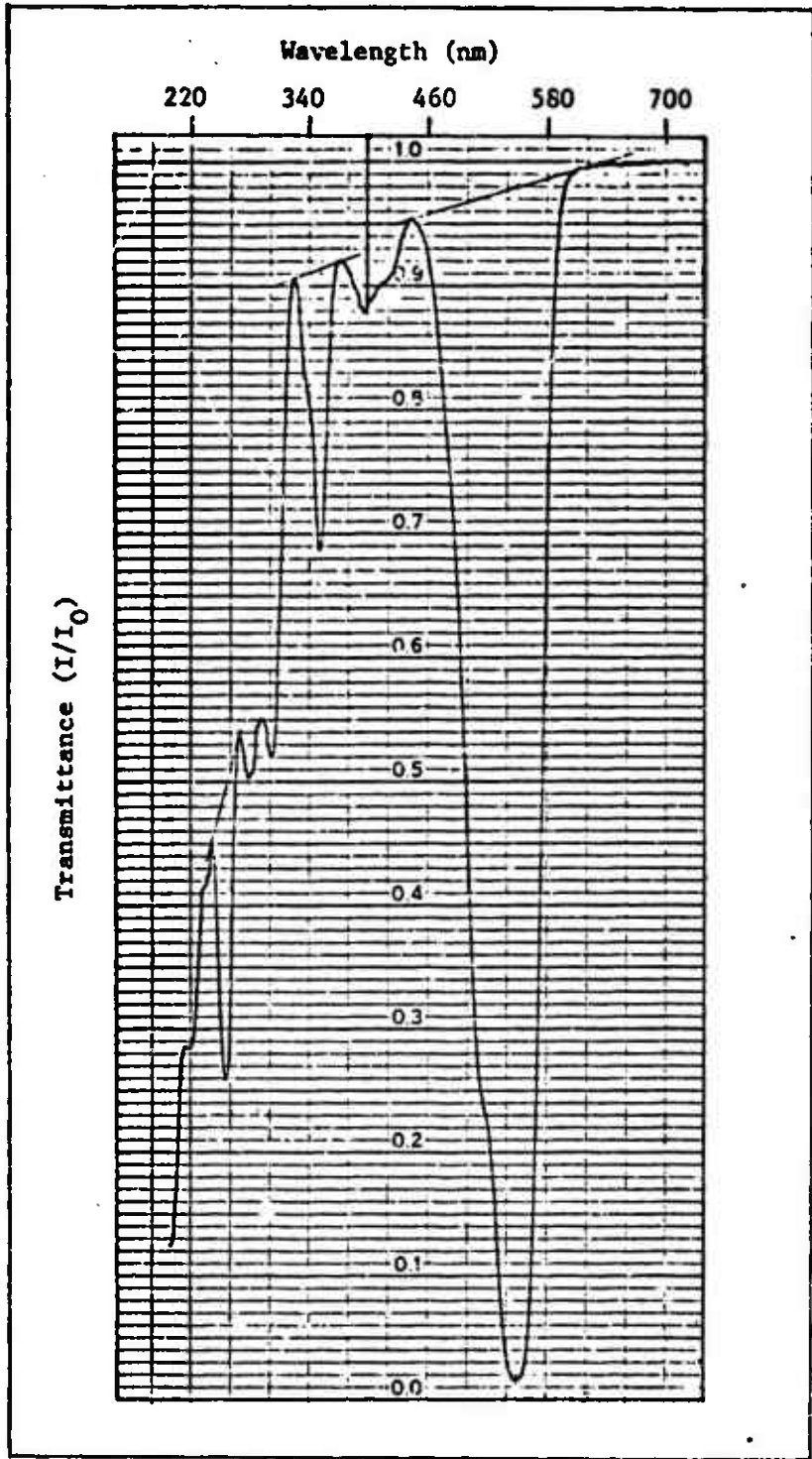
Figure 14

Trial 1, Shot 0 Visible Absorption Spectrum
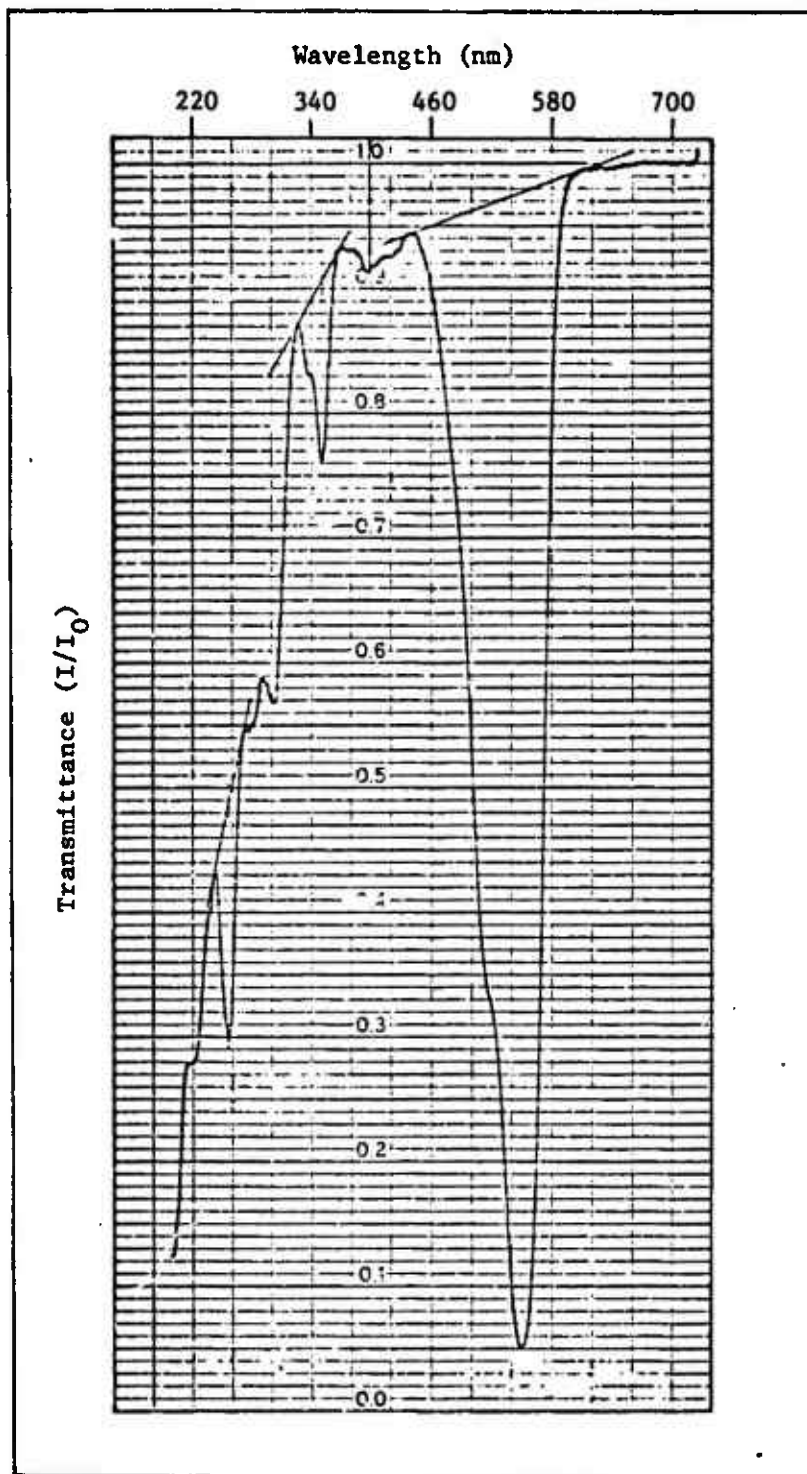
Figure 15

Trial 1, Shot 3000 Visible Absorption Spectrum

estimated to be 0.004. Any variation in the spectra within this amount is most likely due to noise or equipment inaccuracy, but could be the effect of narrow-band absorption differences. Appendix C gives the derivation of absorption coefficients that would result in this amount of an increase in the solution absorption at λ_L. These absorption coefficients were applied to Trial 1 data, and the pulse energies predicted by computer analysis are plotted in Figure 16. The additional plot of theoretical pulse energies in Figure 16 corresponds to a second set of absorption coefficients that were derived so as to provide reduction in output energy consistent with the reduction observed experimentally (these absorption coefficients are listed in Appendix C). To obtain an output energy of 9 millijoules at shot 3000 an absorption coefficient of 1.0 cm^{-1} is required. This corresponds to an I/I_0 value of 0.90; a reduction in transmittance of this magnitude is not indicated by the spectrum in Figure 15. This result suggests that although the absorption of lasing radiation could contribute significantly to the multiplier effect, it would not be solely responsible for the reduction in output energy.

Figure 17 compares the pulse energies calculated for several different rates of lasing and pump radiation absorption that occur simultaneously.

Singlet Quenching by Reaction Products

The final mechanism examined by which the reaction product interferes with laser performance was singlet quenching. From their current studies of KRS degradation, Dr. Schwerzel et al. have proposed the formation of reactive triplets from the upper excited singlet states (Ref 33). In addition to promoting degradation, this triplet formation could

42
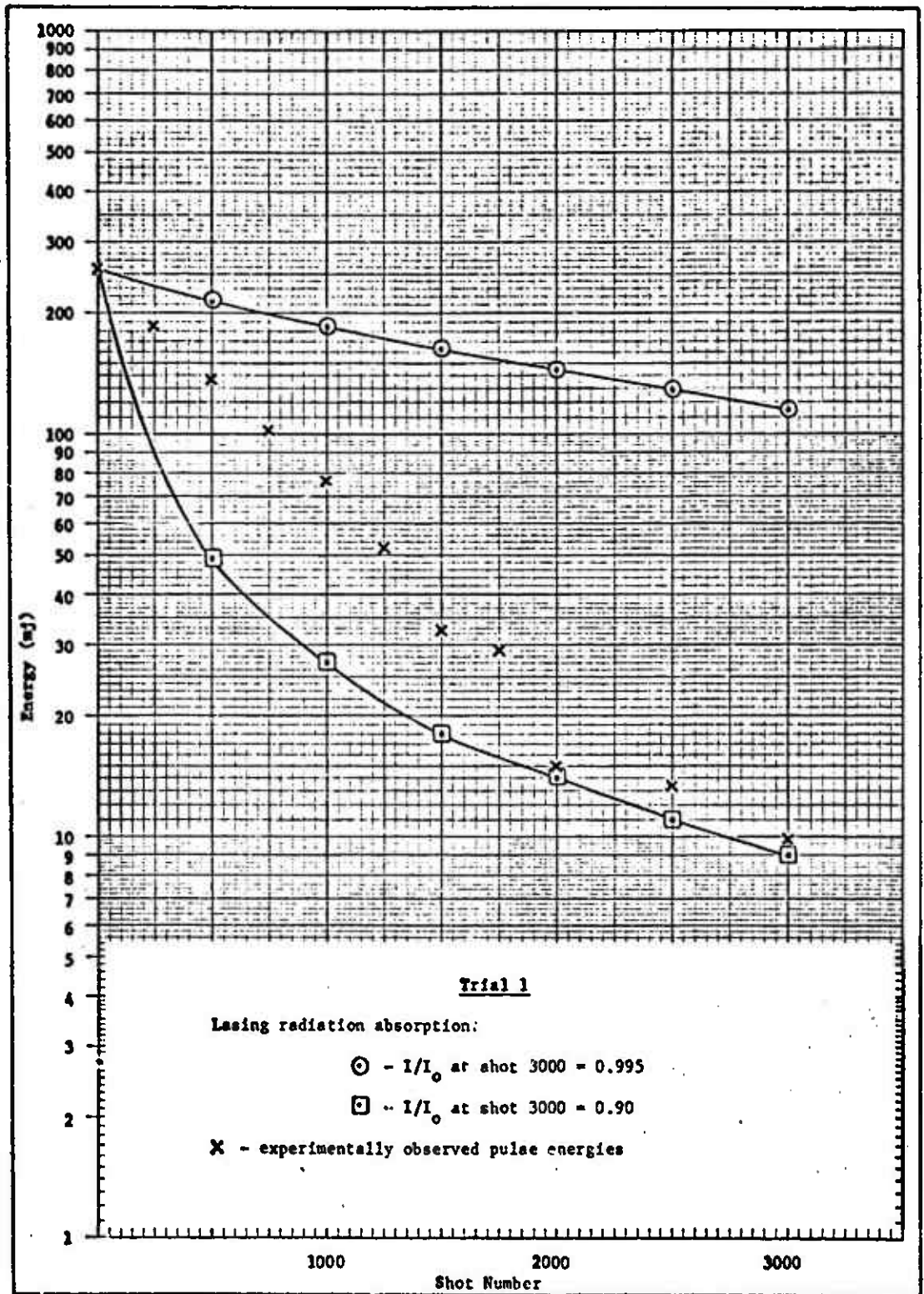
Figure 16

Pulse Energies due to Lasing Radiation Absorption

43
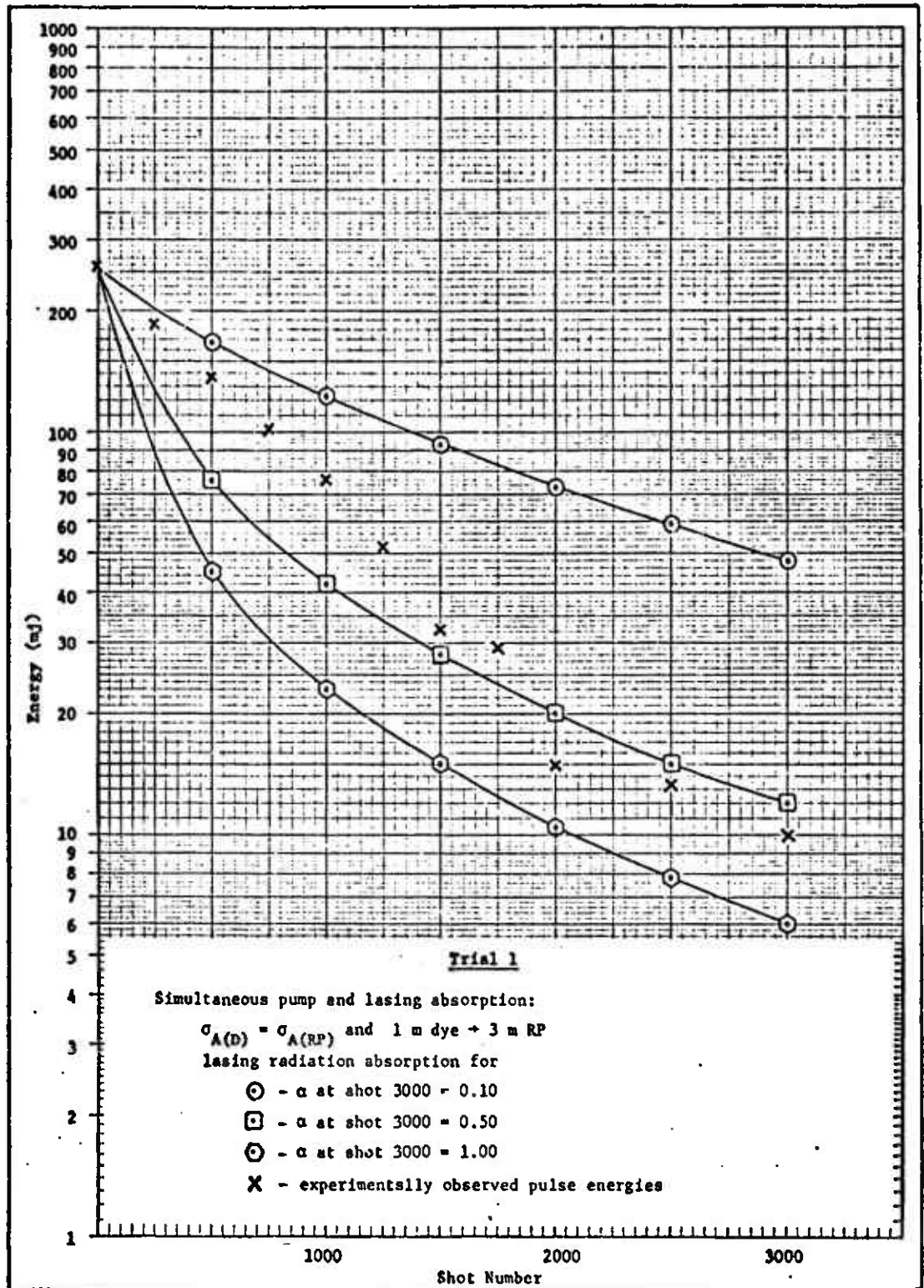
Figure 17

Pulse Energies due to Combined Effects

44
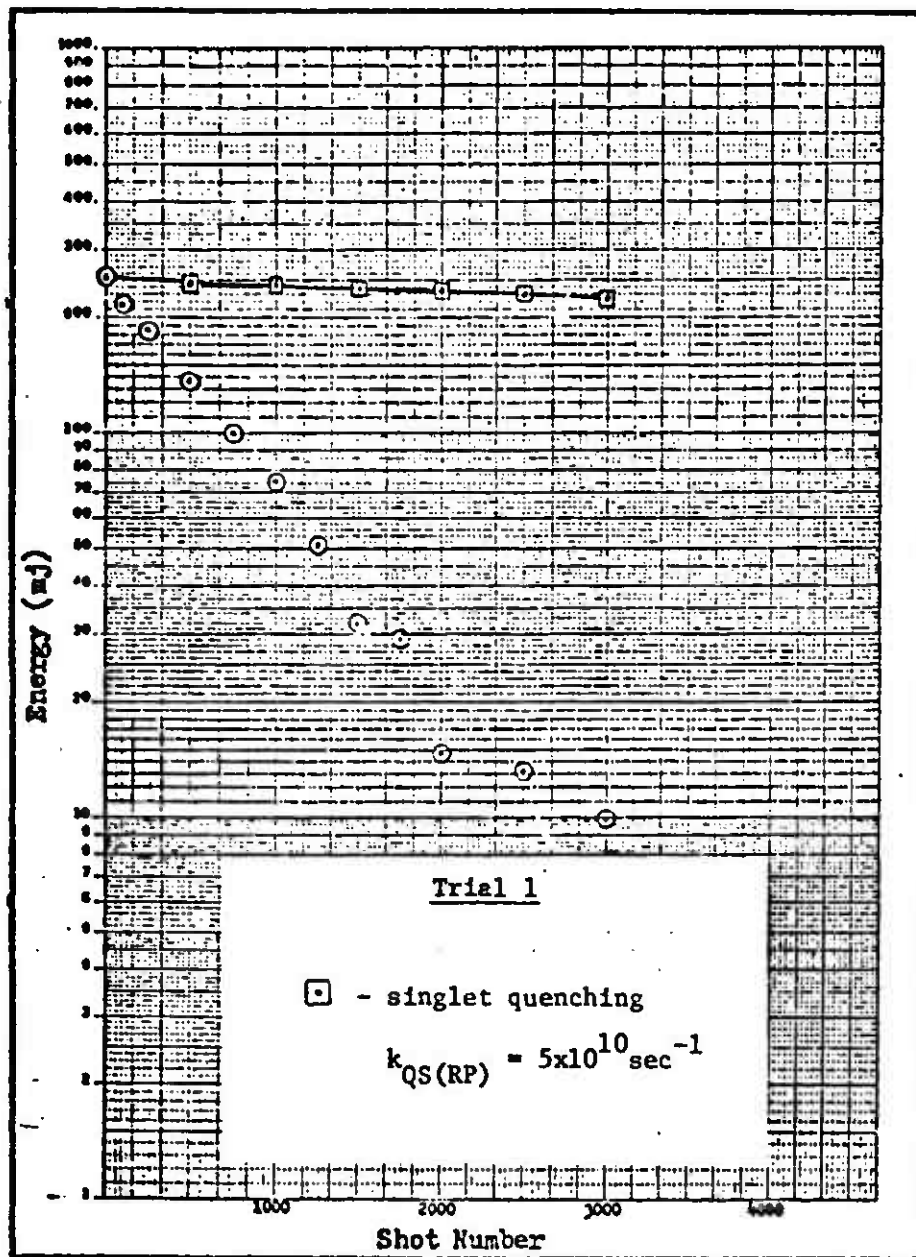
Figure 18

Pulse Energies due to Singlet Quenching by the

Reaction Product

affect the lasing directly by increasing triplet absorption, and would populate the triplet manifold at the expense of the singlet population. The potential of this possibility was assessed by adding an additional term to the rate constants k_{ST} and k_2:

$$k_{ST} = k_{S_1 T_1} + k_{QS} Q_S + k_{QS(RP)} Q_{S(RP)} \qquad (4.6)$$

$$k_2 = k_{S_1 T_1} + k_{S_1 S_0} + k_{QS} Q_S + k_{QS(RP)} Q_{S(RP)} \qquad (4.7)$$

where

$k_{QS(RP)}$ = rate constant for singlet quenching by the reaction product (M^{-1} sec^{-1})

$Q_{S(RP)}$ = concentration of reaction product

The quantity $Q_{S(RP)}$ is the same as c_{RP} introduced previously and has been relabeled to maintain the nomenclature adopted for the rate equations.

The computer program used in the previous analyses was modified to incorporate Eqs (4.6) and (4.7) and to calculate the pulse energy as the reaction product concentration increased; this program is included in Appendix D. Several runs were made for different values of k_{QS}, k_{QT}, and $k_{QS(RP)}$ assuming that 1 molecule of dye produced one molecule of reaction product. The results are presented in Figure 18. One of the more revealing results is the linear decrease in pulse power obtained, which would tend to disqualify this mechanism as the primary cause of the logarithmic multiplier effect. Figure 19 is a comparison of the results from all of the mechanisms tested.

To provide a check on the accuracy of the computer program, W_{max} was estimated from the efficiency of the flashlamp and its spectral output (Appendix F); the value calculated was 1.6×10^{24} photons/sec.
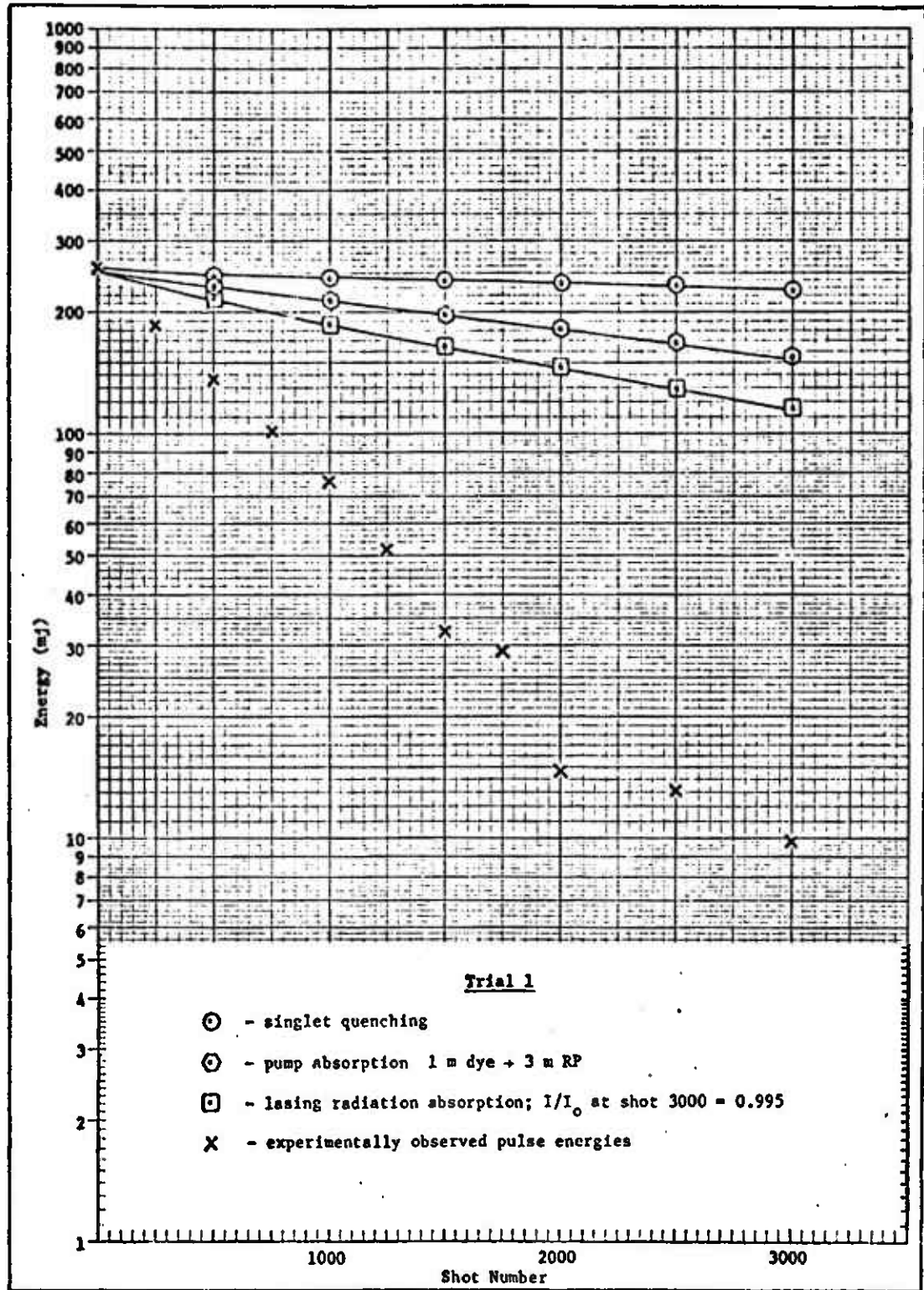
Figure 19

Comparison of Results

47

The value required to set the Trial 1, shot 1 pulse energy equal to 250 mj in all of the preceeding computer analyses was 3.54×10^{24} (photons/sec). This agreement should verify that no major flaws exist in the modeling.

V. Discussion

The computer program that was developed in this study has predicted output energy trends consistent with the known characteristics of the KRS laser and without apparent conflicts quantitatively. Its flexibility has been demonstrated by the ease with which the several variables could be accomodated and singlet quenching by the reaction products could be examined. As the parameters specific to KRS are more accurately determined, the model will be able to effectively predict the relative efficiencies of different operating regimes.

The results from the preceding section show that none of the phenomena that were modeled could account for the magnitude of the multiplier effect using the data available. The most effective mechanism was absorption at the lasing wavelength by the reaction products. Although the half-life for absorption was approximately 2650 shots compared to the demonstrated half-life of 550 shots and was based on the most favorable interpretation of the absorption spectra, the results demonstrate how minute increases in absorption by the dye solution can cause large reductions in the output energy. Both the absorption coefficient corrections and the pump efficiency corrections resulted in non-linear decreases in energy, although they were not logarithmic. In comparison with the experimental data, the theoretical curves for these two phenomena differed enough from the experimental to indicate that another mechanism is responsible, that multiple mechanisms are at work simultaneously, or that the theoretical variable values derived to consider the lasing and pump absorption are inaccurate.

One of the more valuable insights offered by this analysis is the importance of the wavelength of lasing. The parameters δ_S and δ_T are

both functions of λ_L and may vary several orders of magnitude over the excited state singlet and triplet absorption ranges. If triplet absorption ia aignificant at one wavelength, it could be reduced by lasing at a wavelength with a smaller extinction coefficient. The prime consideration in selecting a lasing wavelength would be the absorption band of the reaction product, if this band overlaps the lasing region of the dye.

VI. Conclusions and Recommendations

Conclusions

The analytical model developed to represent the KRS dye laser provides an accurate method of predicting pulse energy decay and relative laser performance as a function of dominant relaxation mechanisms and competitive absorption processes. The generality incorporated into the model enables various potential reaction product effects to be evaluated by simple modification of the power output equation and its associated parameters.

The lack of precise data has prevented this analysis from conclusively identifying the primary phenomena responsible for the multiplier effect.

1. The most effective mechanism of those examined is reaction product absorption at the lasing wavelength.

2. Reaction product absorption at the pump wavelength is a probable factor but is very unlikely to be the primary cause.

3. An increase in intersystem crossing to the triplet manifold due to the formation of reaction products would not produce the logarithmic decrease in energy observed.

4. Mechanisms other than pump and lasing radiation absorption by the reaction products are likely to be responsible for the effect.

Recommendations

The following recommendations are proposed for further study:

1. Repeat the measurement of dye degradation and the corresponding pulse energy decay using KRS in a tunable dye laser. Perform

51

the experiment at several lasing wavelengths within the 630-670 nm region to determine the effect that operation at different wavelengths has on the efficiency and half-life of the laser.

2. Measure the absorption coefficient of the dye solution at the specific lasing wavelength. Accuracy to a minimum of three decimal places is essential. One possible method would be to measure the attenuation of a laser beam tuned to λ_L with a radiometer; this would require a highly stable laser beam to insure the required degree of accuracy. Maximizing the distance traveled by the beam through the dye solution will increase the ratio I/I_0 to provide greater accuracy in calculating the absorption coefficient.

3. Measure the threshold pump power required for each shot in a trial. This quantity will increase if the reaction product is absorbing the pump photons. Any increase in the absorption coefficient found due to lasing absorption by the reaction product must be accounted for first as this also affects the threshold pump power.

4. Run several trials using specific triplet quenching agents such as cyclooctatetraene. If the multiplier effect still occurs this will confirm that it is not attributable to triplet absorption or the loss of molecules to the triplet manifold.

Bibliography

1. Baczynski, A., A. Kossakowski and T. Marszalek. "Dye Laser as a Six-Level System," *Acta Physica Et Chemica* 23(1): 43-47 (1977).

2. -----"Quantum Theory of Dye Lasers," *Zeitschrift Fur Physik B*, B23: 205-212 (1976).

3. -----"Triplet Losses in Dye Lasers," *Zeitschrift Fur Physik B*, B26: 93-95 (1977).

4. Baczynski, A., T. Marszalek and C. Koepke. "Analysis of Nonstationary Solutions of Rate Equations of Dye Laser," *Acta Physica Polonica*, A55: 73-78 (1979).

5. Barrow, Gordon M. *Introduction to Molecular Spectroscopy*. New York: McGraw-Hill Book Company, Inc., 1962.

6. Buettner, A. V., B. B. Snavely, and O. G. Peterson. "Triplet State Quenching of Stimulated Emission from Organic Dye Solutions," *Molecular Luminescence*, edited by E. C. Lim. New York: W. A. Benjamin, Inc., 1969.

7. *CRC Standard Mathematical Tables*, 16th Edition, edited by S. M. Selby. Cleveland: The Chemical Rubber Company, 1968.

8. Dorko, E. A., K. O'Brien and J. Rabins. "Kinetic Studies of Kiton Red S Photodecomposition Under Continuous Working and Flash Photolytic Conditions," *Journal of Photochemistry*, 12: 345-356 (1980).

9. Drake, J. M., R. Morse, R. Steppel, and D. Young. "Kiton Red S and Rhodamine B. The Spectroscopy and Laser Performance of Red Laser Dyes," *Chemical Physics Letters*, 35(2): 181-188 (1 September 1975).

10. Drexhage, K. H. "Structure and Properties of Laser Dyes," *Topics in Applied Physics*, Volume 1 (Second Revised Edition), edited by F. P. Schafer. Berlin: Springer-Verlag, 1977.

11. Gregg, D., M. Querry, J. Marling, S. Thomas, C. Dobler, N. Davies, J. Belew. "Wavelength Tunability of New Flashlamp-Pumped Laser Dyes," *IEEE Journal of Quantum Electronics*, GE-6: 270 (1970).

12. Hammond, P. R. "Effect of Laser Dye Deterioration on Performance," *Applied Physics*, 14: 199-203 (1977).

13. -----"Self-Absorption of Molecular Fluorescence, the Design of Equipment for Measurement of Fluorescence Decay, and the Decay Times of Some Laser Dyes," *Journal of Chemical Physics*, 70(8): 3884-3894 (15 April 1979).

14. Jaffe, H. H. and Milton Orchin. *Theory and Applications of Ultraviolet Spectroscopy*. New York: John Wiley and Sons, Inc., 1964.

15. Johnson, Sidney L. Jr., E. A. Dorko, and G. E. Smith. Degradation of KRS Under Flashed and CW Irradiation. Technical Report AFAL-TR-78-108. Wright-Patterson AFB, Ohio: Air Force Avionica Laboratory, Air Force Wright Aeronautical Laboratories, October 1978.

16. Johnson, Sidney L. Jr. Kiton Red S Lifetime Studies. Technical Report AFAL-TR-77-209, Wright-Patteraon AFB, Ohio: Air Force Avionics Laboratory, Air Force Wright Aeronautical Laboratories, November 1977.

17. Keller, R. A. "Effect of Quenching of Molecular Triplet States in Organic Dye Lasers," IEEE Journal of Quantum Electronics, QE-6(7): 411-416 (July 1970).

18. Levin, M. and M. Snegov. "Effect of Photoreaction Producta on Spontaneous and Stimulated Emission of Alcoholic Solutiona of Rhodamine 6G," Optical Spectroscopy, 38(5): 532-533 (May 1975).

19. Nagaahima, K. and T. Asakura. "Triplet Quenching Effect in Tunable Dye Lasers," Optics Communications, 28(2): 227-232 (February 1979).

20. O'Brien, Kevin, E. A. Dorko, and S. L. Johnson Jr. Kinetic Studies of the Degradation of Kiton Red S Laser Dye. Technical Report AFAL-TR-78-79, Wright-Patterson AFB, Ohio: Air Force Avionics Laboratory, Air Force Wright Aeronautical Laboratories, December 1978.

21. Pappalardo, R., H. Samelson, and A. Lempicki. "Calculated Efficiency of Dye Lasers as a Function of Pump Parameters and Triplet Lifetime," Journal of Applied Physics, 43(9): 3776-3787 (September 1972).

22. Pavlopoulos, T. G. "Prediction of Laser Action Properties of Organic Dyes from their Structure and the Polarization Characteriatics of Their Electronic Transitions," IEEE Journal of Quantum Electronics, QE-9(5): 510-51b (May 1973).

23. Pavlopoulos, T. and P. Hammond. "Spectroscopic Studies of Some Laser Dyes," Journal of the American Chemical Society, 96(21): 6568-6579 (October 16, 1974).

24. Pivovonski, M. and M. Nagel. Tables of Blackbody Radiation Functions. New York: The MacMillan Company, 1961.

25. Rabins, John M., E. A. Dorko and S. L. Johnson Jr. Study of the Correlation Between Degradation of Kiton Red S Laser Dye and Degradation of Laser Energy Under Flash Conditions. Technical Report AFAL-TR-79-1023, Wright-Patterson AFB, Ohio: Air Force Avionics Laboratory, Air Force Wright Aeronautical Laboratories, March 1979.

26. Rabins, John M. Laboratory notes, Book 1, for above experimental study. Dept. of Physics, Air Force Institute of Technology, Wright-Patterson AFB, Ohio: in care of Dr. E. Dorko.

27. Roeas, D. "Giant Pulse Shortening by Resonator Transients," Journal of Applied Physics, 37(5): 2004-2006 (April 1966).

28. Rosenthal, I. "Photochemical Stability of Rhodamine 6G in Solution," Optics Communications, 24(2): 164-166 (February 1978).

29. Sahar, E. and D. Treves. "Excited Singlet-State Absorption in Dyea and Their Effect on Dye Lasers," IEEE Journal of Quantum Electronics, QE-13(12): 962-967 (December 1977).

30. Sahar, E., D. Treves, and I. Wieder. "Fluorescence Quenching in Laser Dyes by Absorption From an Excited Singlet State," Optics Communications, 16(1): 124-127 (January 1976).

31. Schafer, F. P. "Principles of Dye Laser Operation," Topics in Applied Physics, Volume 1 (Second Revised Edition), edited by F. P. Schafer. Berlin: Springer-Verlag, 1977.

32. Schwerzel, Robert E. With Battelle, Columbus Laboratoriea (telephone conversation) September 1980.

33. Schwerzel, R. and N. Edie. "Third Annual Interim Report on Mechanisms of Photochemical Degradation in Xanthene Laser Dyes," Report to USAF Office of Scientific Research. Battelle, Columbus Laboratories; May 29, 1980.

34. Schwerzel, R. and N. Klosterman. "Studies of KRS Photodegradation," Interim research report to USAF Office of Scientific Research. Battelle, Columbus Laboratories, March 10, 1978.

35. Shank, C. V. "Physics of Dye Lasers," Reviews of Modern Physics, 47(3): 649-657 (July 1975).

36. Siegman, A. E. An Introduction to Lasers and Masers. New York: McGraw-Hill Book Company, 1971.

37. Sorokin, P., J. Lankard, V. Moruzzi, and E. Hammond. "Flashlamp-Pumped Organic-Dye Lasers," The Journal of Chemical Physics, 48(10): 4726-4741 (15 May 1968).

38. ----"Laser-Pumped Stimulated Emission From Organic Dyes: Experimental Studies and Analytical Comparisons," IBM Journal, 11: 130-148 (March 1967).

39. Strome, F. C. "The Dye Laser," Eastman Organic Chemical Bulletin, 46(2): 1-9 (1974).

40. Webb, J. P. "Tunable Organic Dye Lasers," Analytical Chemistry, 44(6): 30A-46A (May 1972).

41. Weichel, H. and L. Pedrotti. Staff Notes, Laser Physics I, Department of Physics, Air Force Institute of Technology, Wright-Patterson AFB, Ohio.

42. Wieder, I. "Quenching of Laser Dye Fluorescence by Absorption from an Excited Singlet State," *Applied Physics Letters*, 21(7): 318-320 (1 October 1972).

43. Yariv, Amnon. *Introduction to Optical Electronics*. New York: Holt, Rinehart and Winston, 1976.

Appendix A

Seven-Level Laser Rate Equations

Baczynski et al. (Refs 1-4) have developed a six-level model for dye lasers that incorporates the T_2 level population. The six-level system takes into account triplet absorption but neglects excited state singlet absorption and the possibility of an S_2 population. The equation set
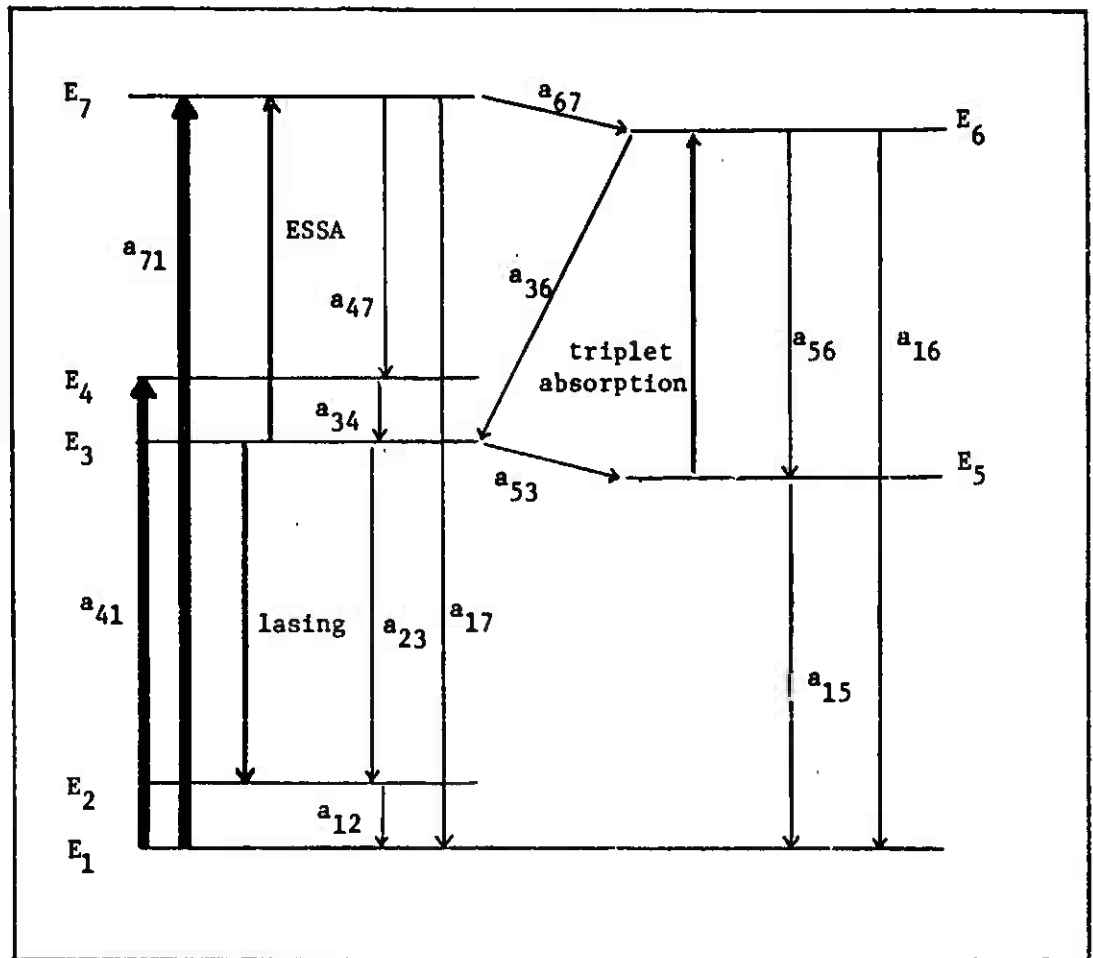
Figure A-1

Seven-Level Laser Model

presented in this appendix is based on the aeven-level model shown in Figure A-1. These rate equations inclue an original one that describes the S_2 (E_7 level) population, and terms appropriate to the S_2 interactions depicted in Figure A-1 have been added to the six-level rate equations. The aeven-level equations are

$$\frac{dn}{dt} = -\frac{n}{\tau_C} + \frac{n}{\tau_{F(R)}}(P_3 - P_2) - \frac{n}{\delta_T \tau_{F(R)}}(P_5 - P_6) - \frac{n}{\delta_S \tau_{F(R)}}(P_3 - P_7) \quad \text{(A.1)}$$

$$\frac{dP_1}{dt} = a_{12}P_2 + a_{15}P_5 + a_{16}P_6 + a_{17}P_7 - (a_{41} + a_{71})P_1 \quad \text{(A.2)}$$

$$\frac{dP_2}{dt} = a_{23}P_3 + \frac{n}{\tau_{F(R)}}(P_3 - P_2) - a_{12}P_2 \quad \text{(A.3)}$$

$$\frac{dP_3}{dt} = a_{34}P_4 + a_{36}P_6 - (a_{53} + a_{23})P_3 - \frac{n}{\tau_{F(R)}}(P_3 - P_2)$$

$$- \frac{n}{\delta_S \tau_{F(R)}}(P_3 - P_7) \quad \text{(A.4)}$$

$$\frac{dP_4}{dt} = a_{41}P_1 + a_{47}P_7 - a_{34}P_4 \quad \text{(A.5)}$$

$$\frac{dP_5}{dt} = a_{53}P_3 - a_{15}P_5 + a_{56}P_6 - \frac{n}{\delta_T \tau_{F(R)}}(P_5 - P_6) \quad \text{(A.6)}$$

$$\frac{dP_6}{dt} = a_{67}P_7 - (a_{56} + a_{16} + a_{36})P_6 + \frac{n}{\delta_T \tau_{F(R)}}(P_5 - P_6) \quad \text{(A.7)}$$

$$\frac{dP_7}{dt} = a_{71}P_1 - (a_{47} + a_{67} + a_{17})P_7 + \frac{n}{\delta_S \tau_{F(R)}}(P_3 - P_7) \quad \text{(A.8)}$$

$$P_1 + P_2 + P_3 + P_4 + P_5 + P_6 + P_7 = 1 \qquad\qquad (A.9)$$

The normalized population density p gives the probability of finding a molecule in a particular level, and Eq (A.9) requires that it can exist only in one of the levels shown in the model. The a_{ij} coefficients are the spontaneous radiation and radiationless transition rates combined; a_{41} and a_{71} are pumping parameters. The remaining terms are consistent with the notation in the main body of the thesis. The numbering of the levels is consistent with the six-level presentation and differs from the numbering system used in the figures in Section III.

Appendix B

Derivation of τ_C and τ_M

Figure B-1 represents the cavity of the dye laser. The gain in intensity of a beam of photons after a round trip through the cavity is

$$I(t + \Delta t) = R_1 R_2 e^{2(\gamma - \alpha)L} I(t) = I(t) + \Delta I(\Delta t) \qquad (B.1)$$

where

$\qquad I(t + \Delta t)$ = resultant intensity after a round trip

$\qquad \Delta t$ = round-trip duration

$\qquad R_1, R_2$ = cavity mirror reflectivities

$\qquad \gamma$ = laser gain coefficient

$\qquad \alpha$ = dye absorption coefficient

$\qquad L$ = length of the medium traversed by the beam

$\qquad I(t)$ = original intensity of beam

$\qquad \Delta I(\Delta t)$ = change in intensity of the beam
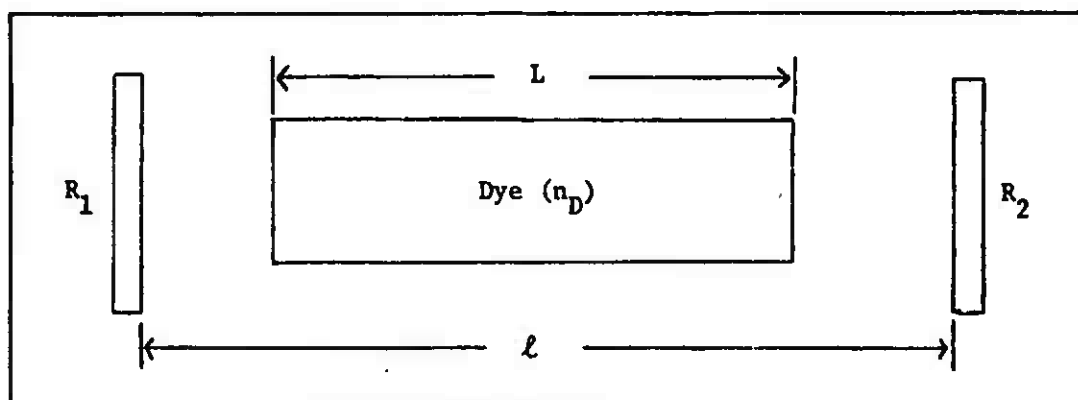
Figure B-1

Laser Cavity Diagram

Dividing Eq (B.1) by I(t) and taking the logarithm of each side we get

$$\ln\left[1 + \frac{\Delta I(\Delta t)}{I(t)}\right] = 2L\left[\gamma - \alpha - \frac{1}{2L}\ln\left(\frac{1}{R_1 R_2}\right)\right] \tag{B.2}$$

For $\Delta I(\Delta t) \ll I(t)$ we can approximate the term $\ln\left(1 + \frac{\Delta I}{I}\right)$ by $\frac{\Delta I}{I}$ to obtain

$$\Delta I = 2L\left[\gamma - \alpha - \frac{1}{2L}\ln\left(\frac{1}{R_1 R_2}\right)\right] I \tag{B.3}$$

The round-trip time Δt is

$$\Delta t = \frac{2n_D L}{c} + \frac{2(\ell - L)}{c} \tag{B.4}$$

where

n_D = index of refraction of the dye solution

c = speed of light in vacuum

ℓ = distance separating the cavity mirrors

Dividing ΔI by Δt and approximating $\frac{\Delta I}{\Delta t}$ by $\frac{dI}{dt}$ we obtain the following differential equation:

$$\frac{dI}{dt} = \frac{cL}{\ell + L(n_D - 1)}\left[\gamma - \alpha - \frac{1}{2L}\ln\left(\frac{1}{R_1 R_2}\right)\right] I \tag{B.5}$$

The number of photons (n) in the beam is directly proportional to the beam intensity, so that the photon rate equation is

$$\frac{dn}{dt} = \frac{cL}{\ell + L(n_D - 1)}\left[\gamma - \alpha - \frac{1}{2L}\ln\left(\frac{1}{R_1 R_2}\right)\right] n \tag{B.6}$$

Without pumping, the gain coefficient γ vanishes and the cavity photons are lost at the rate

$$\frac{dn}{dt} = \frac{cL}{\ell + L(n_D - 1)} \left[- \alpha - \frac{1}{2L}\ln\left(\frac{1}{R_1 R_2}\right) \right] n \qquad (B.7)$$

Integrating Eq (B.7) results in the equation

$$n(t) = n_0 \exp\left(-\frac{t}{\tau_C}\right) \qquad (B.8)$$

where the cavity photon lifetime τ_C is

$$\tau_C = \left\{ \frac{cL}{\ell + L(n_D - 1)} \left[\alpha + \frac{1}{2L}\ln\left(\frac{1}{R_1 R_2}\right) \right] \right\}^{-1} \qquad (B.9)$$

This lifetime characterizes photon losses from the cavity population due to cavity parameters such as the mirror transmissions and absorption by the medium. This can be stated mathematically:

$$\frac{1}{\tau_C} = \frac{1}{\tau_\alpha} + \frac{1}{\tau_{M1}} + \frac{1}{\tau_{M2}} \qquad (B.10)$$

where

τ_α = cavity photon lifetime due to absorption losses

τ_{M1} = cavity photon lifetime due to mirror 1 transmission

τ_{M2} = cavity photon lifetime due to mirror 2 transmission

Eq (B.9) can be factored accordingly:

$$\frac{1}{\tau_C} = \frac{cL}{\ell + L(n_D - 1)} \left[\alpha + \frac{1}{2L}\ln\left(\frac{1}{R_1}\right) + \frac{1}{2L}\ln\left(\frac{1}{R_2}\right) \right] \qquad (B.11)$$

62

Selecting mirror 1 as the transmissive frontal mirror, τ_{M1} becomes τ_M:

$$\tau_M = \left\{ \frac{c}{\ell + L(n_D - 1)} \left[\frac{1}{2} \ln \left(\frac{1}{R_1} \right) \right] \right\}^{-1} \qquad (B.12)$$

The inverse of τ_M gives the rate at which the cavity photons enter into the output beam of the laser. This development has followed the derivation presented by Weichel and Pedrotti (Ref 41:139–141).

Appendix C

Derivation of Values for Π, η', and α

Pump Absorption Factor Π

As the dye degrades, less molecules of dye are available to absorb the pump radiation and lase. To account for the dye reduction the Beer-Lambert Law is used:

$$\frac{I}{I_0} = e^{-\epsilon c d} \qquad (C.1)$$

where

    I = intensity of a beam after passing through an absorbing medium

    I_0 = original intensity of the beam

    ϵ = molar extinction coefficient of the medium at the wavelength

        of the beam

    c = concentration of the absorbing medium

    d = distance traveled through the medium by the beam

The number of photons transmitted per second in a beam of light is directly proportional to the intensity of the beam. Eq (C.1) can then be written

$$\frac{(\rho_0 - \rho)}{\rho_0} = \exp\left(-\epsilon_P c_D d\right) \qquad (C.2)$$

where

    $(\rho_0 - \rho)$ = number of pump photons transmitted per second through

        the medium

    ρ = number of pump photons absorbed per second by the medium

ρ_0 = number of pump photons transmitted per second in the
incident beam

ε_p = molar extinction coefficient for pump absorption

The energy output of the laser should be proportional to ρ; the output
of successive shots can then be adjusted by the factor Π to account for
the loss of dye molecules:

$$\Pi = \frac{\rho}{\rho_1} \tag{C.3}$$

In this equation ρ_1 is the number of photons absorbed per second by shot
1, and ρ is determined for each subsequent shot according to the concen-
tration of dye remaining by using Eq (C.4):

$$\rho = \rho_0 \left[1 - \exp\left(- \varepsilon_p c_D d \right) \right] \tag{C.4}$$

In this case d is the diameter of the dye cavity illuminated by the
flashlamp, and is 0.6 cm (Ref 25:16). The variable Π can now be
expressed as

$$\Pi = \frac{1 - \exp\left(- \varepsilon_p c_D d \right)}{1 - \exp\left(- \varepsilon_p c_{D1} d \right)} \tag{C.5}$$

The term c_{D1} is the concentration of the dye at shot number 1. A typical
cross section for pump absorption is 10^{-16} cm^2; this corresponds to
$\varepsilon_p = 2.60 \times 10^4$ M^{-1}cm^{-1} (Ref 31:33-34). Johnson (Ref 16:70) recorded an
initial output of 352 mj at 10^{-4} M dye and 510 mj to 547 mj at 5×10^{-4} M
dye. Using 350 mj and 530 mj as representative values at these concen-
trations and considering the rate of the ρ values for these shots to be
equal to the ratio of the output energies, ε_p was calculated to be

1.79×10^4 $M^{-1} cm^{-1}$. The values for Π that were used in the computer analysis of lasing without competitive absorption by the reaction product are listed in Table C-I.

Pump Efficiencies η and η'

The number of molecules of reaction product (RP) produced from one dye molecule and the capacity of the reaction product to absorb the pump energy is unknown, although Figure 12 indicates that pump absorption may exist to some extent. To examine competitive absorption by the reaction product its absorption cross section $\sigma_{A(RP)}$ was considered to be equal to the dye absorption cross section $\sigma_{A(D)}$. Since one mole of dye producing two moles of reaction product with $\sigma_{A(D)} = \sigma_{A(RP)}$ is equivalent to one mole of dye producing one mole of reaction product with $\sigma_{A(RP)} = 2\sigma_{A(D)}$, this assumption will still be useful in analyzing the possibility of $\sigma_{A(D)} \neq \sigma_{A(RP)}$.

The total pump efficiency η is a product of several factors; the flashlamp bandwidth, pump photon loss due to mechanisms such as reflection and scattering, and competitive absorption by impurities in the medium. All but the latter factor can be considered constants that can be absorbed into the term W_{max}, as this pump parameter is arbitrarily varied to equate the output energy computed to the experimentally-determined energy of the first shot of the trial being examined. This allows η to be modified to express only the probability that a pump photon will be absorbed by a dye molecule:

$$\eta' = \frac{c_D}{c_D + c_{RP}} \tag{C.6}$$

In addition to introducing η', Π muat reflect the increaae in the number of absorbing moleculea in the medium aa the reaction product replacea the dye. Eq (C.4) can be modified aa follows:

$$\rho = \rho_0 \left\{ 1 - \exp\left[- \epsilon_P (c_D + c_{RP})d \right] \right\}$$ (C.7)

The expreasion for Π than becomes

$$\Pi = \frac{1 - \exp\left[- \epsilon_P (c_D + c_{RP})d \right]}{1 - \exp\left[- \epsilon_P c_{D1} d \right]}$$ (C.8)

The value of Π will be 1.0 for 1 m dye $\rightarrow$ 1 m RP; for the formation of multiple molecules of reaction product per dye molecule Π will be greater than 1.0. The values of η' and Π uaed in Trial 1 for aeveral ratioa of reaction product formation are liated in Table C-II.

Abaorption Coefficient α

To determine the magnitude of the effect that reaction product abaorption at the lasing wavelength could have on the output energy of the laser, molar extinction coefficients at λ_L for the undegraded dye and the reaction product were calculated aaauming that one molecule of dye degraded to produce one molecule of absorbing reaction product. The extinction coefficients were determined using the Beer-Lambert Law in Eq (C.1):

$$\frac{I}{I_0} = e^{-\epsilon c d}$$ (C.1)

Eq (C.1) was modified to consider absorption by both the dye and the reaction product:

$$\frac{I}{I_0} = \exp\left[-\left(\epsilon_D c_D + \epsilon_{RP} c_{RP}\right)d\right] \tag{C.9}$$

whe:e

c_D = concentration of the dye

c_{RP} = concentration of the reaction product

In this application d equals 0.1 cm (Ref 25:22). The absorption coefficient for a specific amount of dye and reaction product can then be obtained directly from the concentrations and the respective extinction coefficients:

$$\alpha = \epsilon_D c_D + \epsilon_{RP} c_{RP} \tag{C.10}$$

For shot 0, Trial 1, I/I_0 was taken to be 0.999, resulting in $\epsilon_D = 51.68$ $M^{-1}cm^{-1}$. The I/I_0 value used for shot 3000 was 0.995, resulting in $\epsilon_{RP} = 1.077 \times 10^3 \ M^{-1}cm^{-1}$. This is equivalent to a cross section for the reaction product of $1.79 \times 10^{-18} cm^2$, which is two orders of magnitude smaller than the $10^{-16} \ cm^2$ values for the ESSA and triplet absorption cross sections. The values for α used in the computer analysis that correspond to the above amount of transmittance are listed in Table C-III. Table C-IV lists the absorption coefficients that produce pulse decay comparable to the observed experimental decay. Table C-V tabulates the values used for Π, η, and α that produced the pulse energies plotted in Figure 17.

Table C-I

Dye Concentration Corrections

Trial	Shot Number	c_D ($\times 10^{-4}$ M)	Π
1	1	1.935	1.0000
	500	1.870	0.9897
	1000	1.805	0.9786
	1500	1.740	0.9667
	2000	1.675	0.9539
	2500	1.610	0.9402
	3000	1.545	0.9256
2	1	1.960	1.0000
	500	1.922	0.9942
	1000	1.884	0.9882
	1500	1.846	0.9819
	2000	1.808	0.9754
	2500	1.770	0.9686
	3000	1.732	0.9615
3	1	2.000	1.0000
	500	1.964	0.9948
	1000	1.928	0.9894
	1500	1.892	0.9837
	2000	1.856	0.9779
	2500	1.820	0.9718
	3000	1.784	0.9655

$$\epsilon_p = 1.79 \times 10^4 \text{ M}^{-1}\text{cm}^{-1}$$

$$d = 0.6 \text{ cm}$$

69

Table C-II

Competitive Pump Absorption Corrections

Trial	Shot Number	c_D ($\times 10^{-4}$ M)	c_{RP} ($\times 10^{-4}$ M)	Π	η'
1 molecule dye → 1 molecule RP					
1	1	1.935	0	1.0	1.0000
	500	1.870	0.065	1.0	0.9664
	1000	1.805	0.130	1.0	0.9328
	1500	1.740	0.195	1.0	0.8992
	2000	1.675	0.260	1.0	0.8656
	2500	1.610	0.325	1.0	0.8320
	3000	1.545	0.390	1.0	0.7984
1 molecule dye → 2 molecules RP					
1	1	1.935	0	1.0	1.0000
	500	1.870	0.130	1.0096	0.9350
	1000	1.805	0.260	1.0186	0.8741
	1500	1.740	0.390	1.0270	0.8169
	2000	1.675	0.520	1.0349	0.7631
	2500	1.610	0.650	1.0422	0.7124
	3000	1.545	0.780	1.0490	0.6645
1 molecule dye → 3 molecules RP					
1	1	1.935	0	1.0	1.0000
	500	1.870	0.195	1.0186	0.9056
	1000	1.805	0.390	1.0349	0.8223
	1500	1.740	0.585	1.0490	0.7484
	2000	1.675	0.780	1.0612	0.6823
	2500	1.610	0.975	1.0719	0.6228
	3000	1.545	1.170	1.0812	0.5691

$$\epsilon_p = 1.79 \times 10^4 \ M^{-1}cm^{-1}$$

$$d = 0.6 \ cm$$

Table C-III

Absorption Coefficients:

I/I_0 at shot 3000 = 0.995

Trial	Shot Number	c_D (x10^{-4}M)	$\varepsilon_D c_D$ (cm^{-1})	c_{RP} (x10^{-4}M)	$\varepsilon_{RP} c_{RP}$ (cm^{-1})	α (cm^{-1})
1	1	1.935	0.01	0	0	0.01000
	500	1.870	0.00966	0.065	0.00700	0.01666
	1000	1.805	0.00933	0.130	0.01401	0.02334
	1500	1.740	0.00899	0.195	0.02101	0.03000
	2000	1.675	0.00866	0.260	0.02802	0.03668
	2500	1.610	0.00832	0.325	0.03502	0.04334
	3000	1.545	0.00798	0.390	0.04203	0.05001
2	1	1.960	0.01013	0	0	0.01013
	500	1.922	0.00993	0.038	0.00409	0.01402
	1000	1.884	0.00974	0.076	0.00819	0.01793
	1500	1.846	0.00954	0.114	0.01228	0.02182
	2000	1.808	0.00934	0.152	0.01638	0.02572
	2500	1.770	0.00915	0.190	0.02047	0.02962
	3000	1.732	0.00895	0.228	0.02457	0.03352
3	1	2.000	0.01034	0	0	0.01034
	500	1.964	0.01015	0.036	0.00388	0.01403
	1000	1.928	0.00996	0.072	0.00776	0.01772
	1500	1.892	0.00978	0.108	0.01164	0.02142
	2000	1.856	0.00959	0.144	0.01552	0.02511
	2500	1.820	0.00941	0.180	0.01940	0.02881
	3000	1.784	0.00922	0.216	0.02328	0.03250

$$\varepsilon_D = 51.68 \ M^{-1}cm^{-1}$$

$$\varepsilon_{RP} = 1.077 \times 10^3 \ M^{-1}cm^{-1}$$

$$d = 0.1 \ cm$$

Table C-IV

Absorption Coefficients:

I/I_0 at shot 3000 = 0.90

Trial	Shot Number	c_D $(\times 10^{-4}\text{M})$	$\epsilon_D c_D$ (cm^{-1})	c_{RP} $(\times 10^{-4}\text{M})$	$\epsilon_{RP} c_{RP}$ (cm^{-1})	α (cm^{-1})
1	1	1.935	0.01000	0	0	0.01000
	500	1.870	0.00966	0.065	0.16536	0.17502
	1000	1.805	0.00933	0.130	0.33072	0.34005
	1500	1.740	0.00899	0.195	0.49608	0.50507
	2000	1.675	0.00866	0.260	0.66144	0.67010
	2500	1.610	0.00832	0.325	0.82680	0.83512
	3000	1.545	0.00798	0.390	0.99216	1.00014

$$\epsilon_D = 51.68 \ \text{M}^{-1}\text{cm}^{-1}$$

$$\epsilon_{RP} = 2.544 \times 10^{14} \ \text{M}^{-1}\text{cm}^{-1}$$

$$d = 0.1 \ \text{cm}$$

Table C-V

Variable Values for Plots in Figure 17

Trial	Shot Number	α (cm^{-1})	Π	η	
1	1	0.01000	1.0000	1.0000	
	500	0.02500	1.0186	0.9056	$\epsilon_D = 51.68\ M^{-1}cm^{-1}$
	1000	0.04001	1.0349	0.8223	
	1500	0.05501	1.0490	0.7484	$\epsilon_{RP} = 0.236 \times 10^4\ M^{-1}cm^{-1}$
	2000	0.07002	1.0612	0.6823	
	2500	0.08502	1.0719	0.6228	
	3000	0.10002	1.0812	0.5691	
1	1	0.01000	1.0000	1.0000	
	500	0.09169	1.0186	0.9056	
	1000	0.17339	1.0349	0.8223	$\epsilon_D = 51.68\ M^{-1}cm^{-1}$
	1500	0.25508	1.0490	0.7484	
	2000	0.33678	1.0612	0.6823	$\epsilon_{RP} = 1.262 \times 10^4\ M^{-1}cm^{-1}$
	2500	0.41847	1.0719	0.6228	
	3000	0.50016	1.0812	0.5691	
1	1	0.01000	1.0000	1.0000	
	500	0.17502	1.0186	0.9056	
	1000	0.34005	1.0349	0.8223	$\epsilon_D = 51.68\ M^{-1}cm^{-1}$
	1500	0.50507	1.0490	0.7484	
	2000	0.67010	1.0612	0.6823	$\epsilon_{RP} = 2.544 \times 10^4\ M^{-1}cm^{-1}$
	2500	0.83512	1.0719	0.6228	
	3000	1.00014	1.0812	0.5691	

Appendix D

Computer Programs for Computing Pulae Energies

Two computer programs are used in the analysis. Program 1 is used with the variables Π, η^*, and α. Program 2 considers η^* and α constant and maintains Π as a variable. This program requires the concentration of the reaction product to be input for each shot and ia designed to calculate output energy for various rates of singlet quenching by the reaction product. A provision for triplet quenching in addition to the singlet quenching has been included. For the analysis results given in Section IV triplet quenching by the reaction product was negated by aetting the triplet quenching rate constant $k_{QT(RP)} = 0$.

Three constants (C1, C2, and C3) must be input as data. These are specific to the laser geometry and are the same for both programs:

$$C1 = h\nu_L \left[\frac{c}{2\ell + 2L(n_D - 1)} \right] \ln \left(\frac{1}{R_1} \right) \qquad (D.1)$$

$$C2 = \frac{cL}{\ell + L(n_D - 1)} \qquad (D.2)$$

$$C3 = \frac{1}{2L} \ln \left(\frac{1}{R_1 R_2} \right) \qquad (D.3)$$

The parameters and variables correspond as follows:

N = number of intervals desired to divide the pulse into for the purpose of the trapezoidal approximation

$\text{WMAX} = W_{max}$

$\text{TAUFR} = \tau_{F(R)}$

$\text{TAUPR} = \tau_{P(R)}$

$\text{DELS} = \delta_S$

$$\text{DELT} = \delta_T$$

$$\text{KS1S0} = k_{S_1 S_0}$$

$$\text{KS1T1} = k_{S_1 T_1}$$

$$\text{KT1S0} = k_{T_1 S_0}$$

$$\text{QS} = Q_S$$

$$\text{QT} = Q_T$$

$$\text{KQS} = k_{QS}$$

$$\text{KQT} = k_{QT}$$

$$\text{ABS} = \alpha$$

$$\text{PCTG} = \Pi$$

$$\text{ETA} = \eta'$$

$$\text{KQSRP} = k_{QS(RP)}$$

$$\text{KQTRP} = k_{QT(RP)}$$

$$\text{RP} = \text{concentration of reaction product (M)}$$

Data Input (Program 1)

    CARD 1: N, C1, C2, C3, WMAX

           Note: WMAX is selected to adjust the shot 1 energy to the

           desired value.

    CARD 2: TAUFR, TAUPR, DELS, DELT, KS1S0, KS1T1, KT1S0

The first two cards above establish the parameter values used in
the computer analysis. Sets of cards must be assembled for the
specific shots of each trial aa follows:

    CARD A: TRIAL, NR

           Use any convenient tag number to designate each trial;

use a negative number if a plot is not desired. NR is
the number of shot data cards submitted in the trial
(excluding the final dummy card).

CARD B: QS, QT, KQS, KQT

Input the parameter values applicable to the trial; this
card inputs data for singlet and triplet quenching such
as when oxygen is in solution.

CARD C → ?: SHOTNR, ABS, PCTG, ETA

One card will be submitted for each shot examined during
the trial. These cards input the variable values for each
shot. The card following the last shot card is a dummy
card with a negative ABS value (I use 9999,-1,9999,9999).

If additional trials are to be analyzed, begin each new set with
Cards A and B (applicable to the conditions in the new trial) and
be sure to end each set with the dummy data card. After the final
data card in the last trial (this will be the dummy card) the final
card in the data stack will be 0,0 (see the comment on line 28 of
the program readout).

The computer printout will be self-explanatory.

PROGRAM 1

```
1          PROGRAM LASER (INPUT, OUTPUT)
           REAL LN2,KOS,KOT,KS1S0,KS1T1,KT1S0,K2,KT,KST,NPHOT
           INTEGER SHOTNR
           DIMENSION T(1000),P(10000),NPHOT(1000)
5          DIMENSION E(20),SHOT(20),WDTH(20),AB(20),PCT(20),TAUC(20),QRE(20)
           READ*,N,C1,C2,C3,WMAX
C WMAX IS SELECTED TO EQUATE THE SHOT 1 ENERGY TO EXPERIMENTAL VALUES
           READ*,TAUFR,TAUPR,OELS,OELT,KS1S0,KS1T1,KT1S0
C THESE PARAMETERS ARE CONSIDERED TO BE CONSTANTS
10             PRINT*,"               "
               PRINT*,"        "
               PRINT*,"        "
               PRINT*,"        "
               PRINT*,"VARIABLE W/SHOTNR: ABS, ETA, PCTG"
15             PRINT*,"ASSUMPTION:  KT*TAUPR>>1"
               PRINT*,"NEGATIVE TRIAL NOS WILL NOT BE GRAPHED"
               PRINT*,"        "
               PRINT*,"        "
               PRINT*,"WMAX = ",WMAX
20             PRINT*,"OELS = ",OELS," OELT = ",OELT
               PRINT*,"KS1S0 = ",KS1S0," KS1T1 = ",KS1T1
               PRINT*,"KT1S0 = ",KT1S0
               PRINT*,"        "
               PRINT*,"        "
25             PRINT*,"        "
4          READ*,TRIAL,NR
C IF A PLOT IS NOT REQUIRED USE A NEGATIVE TRIAL NUMBER
C THE FINAL DATA CARD SHOULD BE1 0,0  (SEE NEXT COMMAND)
           IF (TRIAL.EQ.1.) GO TO 5
30         READ*,OS,OT,KOS,KOT
C KOS AND KOT WILL DEPEND UPON THE SPECIFIC QUENCHING AGENT
           K2=KOS*OS+KS1T1+KS1S0
           KST=KOS*OS+KS1T1
           KT=KOT*OT+KT1S0
35         TAUF=1/(1/TAUFR+K2)
           TAUP=1/(1/TAUPR+KT)
           PHI=TAUF/TAUFR
           ASSUMP=KT*TAUPR
           PRINT*,"TRIAL NO = ",TRIAL
40         PRINT*,"KT*TAUPR = ",ASSUMP
C THE ABOVE PRINTOUT WILL CONFIRM THE VALIDITY OF THE ASSUMPTION, LINE 15
               PRINT*,"SINGLET QUENCHING RATE CONSTANT (KOS) = ",KOS
               PRINT*,"TRIPLET QUENCHING RATE CONSTANT (KOT) = ",KOT
               PRINT*,"SINGLET QUENCHER CONCENTRATION (OS) = ",OS
45             PRINT*,"TRIPLET QUENCHER CONCENTRATION (OT) = ",OT
               PRINT*,"        "
               PRINT*,"        "
               PRINT*,"        "
               PRINT*,"        "
50             PRINT*,"K2 = ",K2
               PRINT*,"KST = ",KST
               PRINT*,"KT = ",KT
               PRINT*,"FLUORESCENCE LIFETIME (TAUF) = ",TAUF
               PRINT*,"PHOSPHORESCENCE LIFETIME (TAUP) = ",TAUP
55             PRINT*,"QUANTUM FLUORESCENCE (PHI) = ",PHI
C THE ABOVE VALUES INDICATE WHETHER THE PARAMETER VALUES ARE REASONABLE
               PRINT*,"        "
               PRINT*,"        "
               PRINT*,"        "
60         C4=(OELS*OELT*KT-OELT*KT-KST*OELS)/(OELS*OELT*KT)
           LN2=ALOG(2.)
           ICASE=0
2          READ*,SHOTNR,ABS,PCTG,ETA
           IF (ABS.LT.0.)GO TO 10
65 C PLACE DUMMY DATA CARD WITH NEGATIVE ABS AT END OF THE TRIALS DATA CARDS
```

77

```
              ICASE=ICASE+1
              SHOT(ICASE)=SHOTNR
              AC(ICASE)=ABS
              PCT(ICASE)=PCTG
70            OPE(ICASE)=ETA
              TAUC(ICASE)=1/(C2*(ABS+C3))
              WPTH(ICASE)=1./ETA/PHI/TAUC(ICASE)/C4
              E(ICASE)=0.
              OT=5E-7/(N-1)
75    C THE FOLLOWING LOOP COMPUTES THE ENERGY IN THE PULSE
              DO 1I=1,N
              T(I)=-2.5E-7+(I-1)*OT
              WP=WMAX*EXP(-LN2*(T(I)**2)/(5E-7**2))
              NPHOT(I)=WP*TAUC(ICASE)*ETA*C4*PCTG
80            P(I) = C1*NPHOT(I)
              F=1.
              IF (I.EQ.1.OR.I.EQ.N)F=0.5
              E(ICASE)=E(ICASE)+F*P(I)*OT
      1'      CONTINUE
85            PRINT*,"FOR SHOT NO ",SHOTNR," ENERGY = ",E(ICASE)
              PRINT*,"           THRESHOLD PUMP POWER (WPTH) = ",WPTH(ICASE)
              PRINT*,"     .     PHOTON CAVITY LIFETIME (TAUC) = ",TAUC(ICASE)
              PRTNT*,"     "
              GO TO 2
90    10      PRINT*,"     "
              PRINT*,"     "
              PRINT*,"     "
      C THIS LOOP PRINTS OUT THE VARIABLE VALUES USED IN THE TRIAL
              DO 3ICASE=1,NR
95            PRINT*,"SHOT ",SHOT(ICASE)," ABS ",AC(ICASE)," PCTG ",PCT(ICASE),
             &" ETA ",OPE(ICASE)
      3       CONTINUE
              PRINT*,"     "
              PRINT*,"     "
100           PRINT*,"     "
              IF (TRIAL.LT.1.) GO TO 4
      C THE ABOVE STATEMENT ALLOWS BYPASSING THE PLOT SEQUENCE
              CALL DRAWZ(SHOT,E,WPTH,P,T,-2,1,NR,3,-1)
              PRINT*,"     "
105           PRINT*,"     "
              PRINT*,"     "
              GO TO 4
      5       STOP
              ENO
```

78

```
1          PROGRAM LASER (INPUT, OUTPUT)
           REAL LN2,KOS,KOT,KS1S0,KS1T1,KT1S0,K2,KT,KST,NPHOT,KOSRP,KQTRP
           INTEGER SHOTNR
           DIMENSION T(1100),P(10000),NPHOT(1000)
5          DIMENSION E(20),SHOT(20),WPTH(20),PCT(20),RPC(20)
           READ*,N,C1,C2,C3,WMAX
C WMAX IS SELECTED TO EQUATE THE SHOT 1 ENERGY TO EXPERIMENTAL VALUES
           READ*,TAUFR,TAUPR,DELS,DELT,KS1S0,KS1T1,KT1S0,ABS,ETA
C THE ABOVE PARAMETERS ARE CONSIDERED TO BE CONSTANTS
10         TAUC=1/(C2*(ABS+C3))
           PRINT*,"                "
           PRINT*,"                "
           PRINT*,"                "
15         PRINT*,"ASSUMPTION: KT*TAUPR>>1"
           PRINT*,"NEGATIVE TRIAL NOS WILL NOT BE GRAPHED"
           PRINT*,"                "
           PRINT*,"                "
           PRINT*,"WMAX = ",WMAX
20         PRINT*,"ABS = ",ABS," ETA = ",ETA
           PRINT*,"DELS = ",DELS," DELT = ",DELT
           PRINT*,"KS1S0 = ",KS1S0," KS1T1 = ",KS1T1
           PRINT*,"KT1S0 = ",KT1S0
           PRINT*,"                "
25         PRINT*,"                "
           PRINT*,"                "
4          READ*,TRIAL,NR
C IF A PLOT IS NOT REQUIRED USE A NEGATIVE TRIAL NUMBER
C THE FINAL DATA CARD SHOULD BE: 0,0   (SEE NEXT COMMAND)
30         IF (TRIAL.EQ.0.) GO TO 5
           READ*,OS,OT,KOS,KOT,KOSRP,KQTRP
           PRINT*,"TRIAL NO = ",TRIAL
           PRINT*,"SINGLET QUENCHING RATE CONSTANT (KOS) = ",KOS
           PRINT*,"TRIPLET QUENCHING RATE CONSTANT (KOT) = ",KOT
35         PRINT*,"RATE CONSTANT FOR SINGLET QUENCHING BY RP = ",KOSRP
           PRINT*,"RATE CONSTANT FOR TRIPLET QUENCHING BY RP = ",KQTRP
           PRINT*,"SINGLET QUENCHER CONCENTRATION (OS) = ",OS
           PRINT*,"TRIPLET QUENCHER CONCENTRATION (OT) = ",OT
           PRINT*,"                "
40         PRINT*,"                "
           PRINT*,"                "
           PRINT*,"                "
           LN2=ALOG(2.)
           ICASE=0
45   2     READ*,SHOTNR,PCTG,RP
           IF (SHOTNR.LT.0.)GO TO 10
C PLACE DUMMY DATA CARD WITH NEGATIVE SHOTNR AT END OF THE TRIALS DATA CARDS
           K2=KOS*OS+KS1T1+KS1S0+KQSRP*RP
           KST=KOS*OS+KS1T1+KOSRP*RP
50         KT=KOT*OT+KT1S0
           C4=(DELS*DELT*KT-DELT*KT-KST*DELS)/(DELS*DELT*KT)
           TAUP=1/(1/TAUPR+KT)
           TAUF=1/(1/TAUFR+K2)
           PHI=TAUF/TAUFR
55         ICASE=ICASE+1
           SHOT(ICASE)=SHOTNR
           RPC(ICASE)=RP
           PCT(ICASE)=PCTG
           WPTH(ICASE)=1./ETA/PHI/TAUC*C4
60         E(ICASE)=0.
           OT=3E-7/(N-1)
C THE FOLLOWING LOOP COMPUTES THE ENERGY IN THE PULSE
           DO 1I=1,N
           T(I)=-2.5E-7+(I-1)*OT
```

```
65          WP=WMAX*EXP(-LN2*(T(I)**2)/(5E-7**2))
            NPHOT(I)=WP*TAUC*ETA*C4*PCTS
            P(I) = C1*NPHOT(I)
            F=1.
            IF (I.EQ.1.OR.I.EQ.N)F=0.5
70          E(ICASE)=E(ICASE)+F*P(I)*DT
      1     CONTINUE
            PRINT*,"FOR SHOT NO ",SHOTNR," ENERGY = ",E(ICASE)
            PRINT*,"           THRESHOLD PUMP POWER (WPTH) = ",WPTH(ICASE)
            PRINT*,"K2 = ",K2
75          PRINT*,"KST = ",KST
            PRINT*,"KT = ",KT
            PRINT*,"KT*TAUPR = ",ASSUMP
C THE ABOVE PRINTOUT WILL CONFIRM THE VALIDITY OF THE ASSUMPTION
            PRINT*,"FLUORESCENCE LIFETIME (TAUF) = ",TAUF
80          PRINT*,"PHOSPHORESCENCE LIFETIME (TAUP) = ",TAUP
            PRINT*,"QUANTUM FLUORESCENCE (PHI) = ",PHI
            PRINT*,"       "
            PRINT*,"       "
            PRINT*,"       "
85          GO TO 2
      10    PRINT*,"       "
            PRINT*,"       "
            PRINT*,"       "
C THIS LOOP PRINTS OUT THE VARIABLE VALUES USED IN THE TRIAL
90          DO 3ICASE=1,NR
            PRINT*,"SHOT ",SHOT(ICASE)," PCTS ",PCT(ICASE)," RP ",RPC(ICASE)
      3     CONTINUE
            PRINT*,"       "
            PRINT*,"       "
95          PRINT*,"       "
            IF (TRIAL.LT.0.) GO TO 4
C THE ABOVE STATEMENT ALLOWS BYPASSING THE PLOT SEQUENCE
            CALL DRAWZ(SHOT,E,WPTH,P,T,-2,1,NR,1,-1)
            PRINT*,"       "
100         PRINT*,"       "
            PRINT*,"       "
            GO TO 4
      5     STOP
            END
```

80

Appendix E

Dye Degradation and Pulse Decay Data

The following graphs have been reproduced from Figures 13-18,
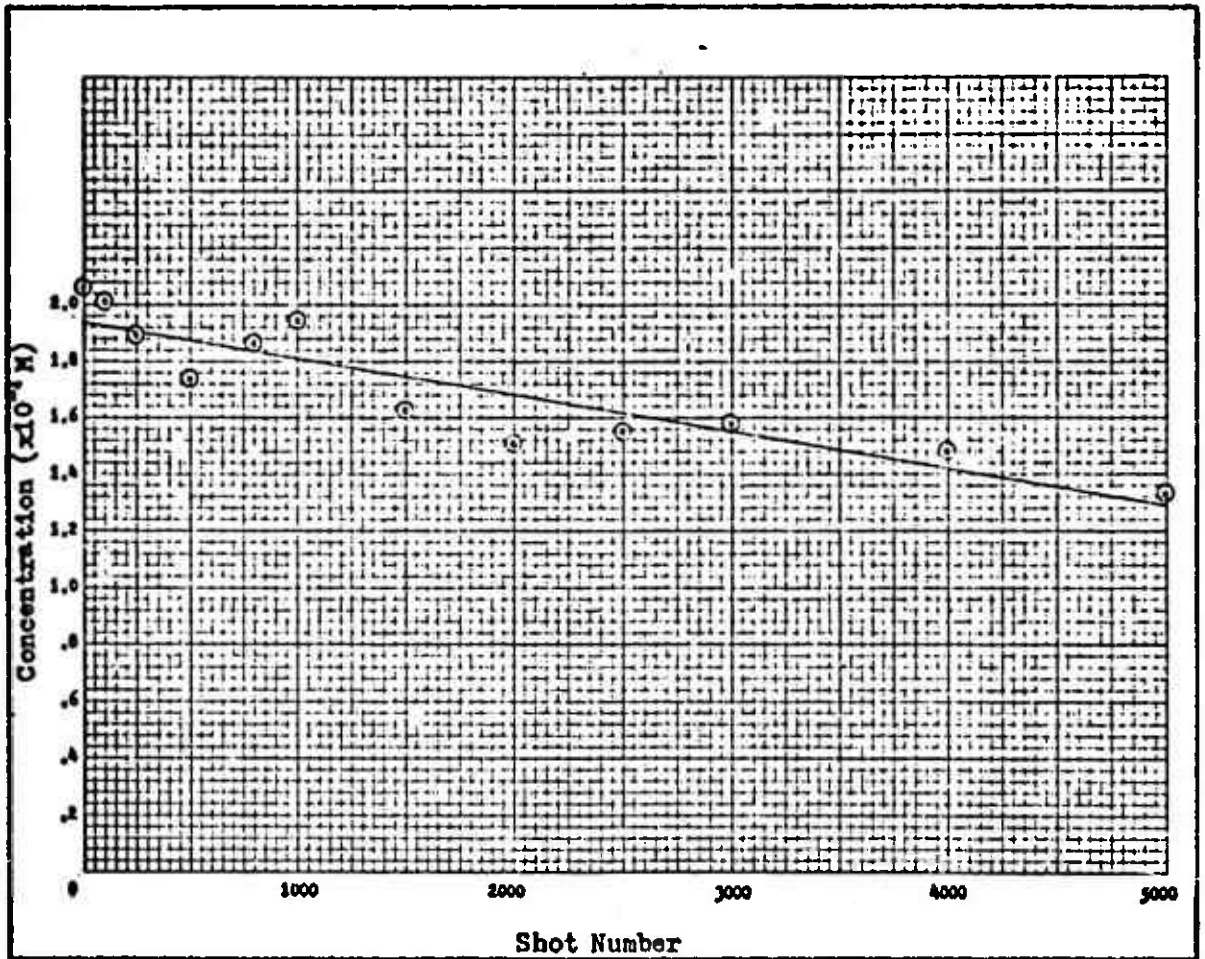Ref 25:30-35.

Figure E-1

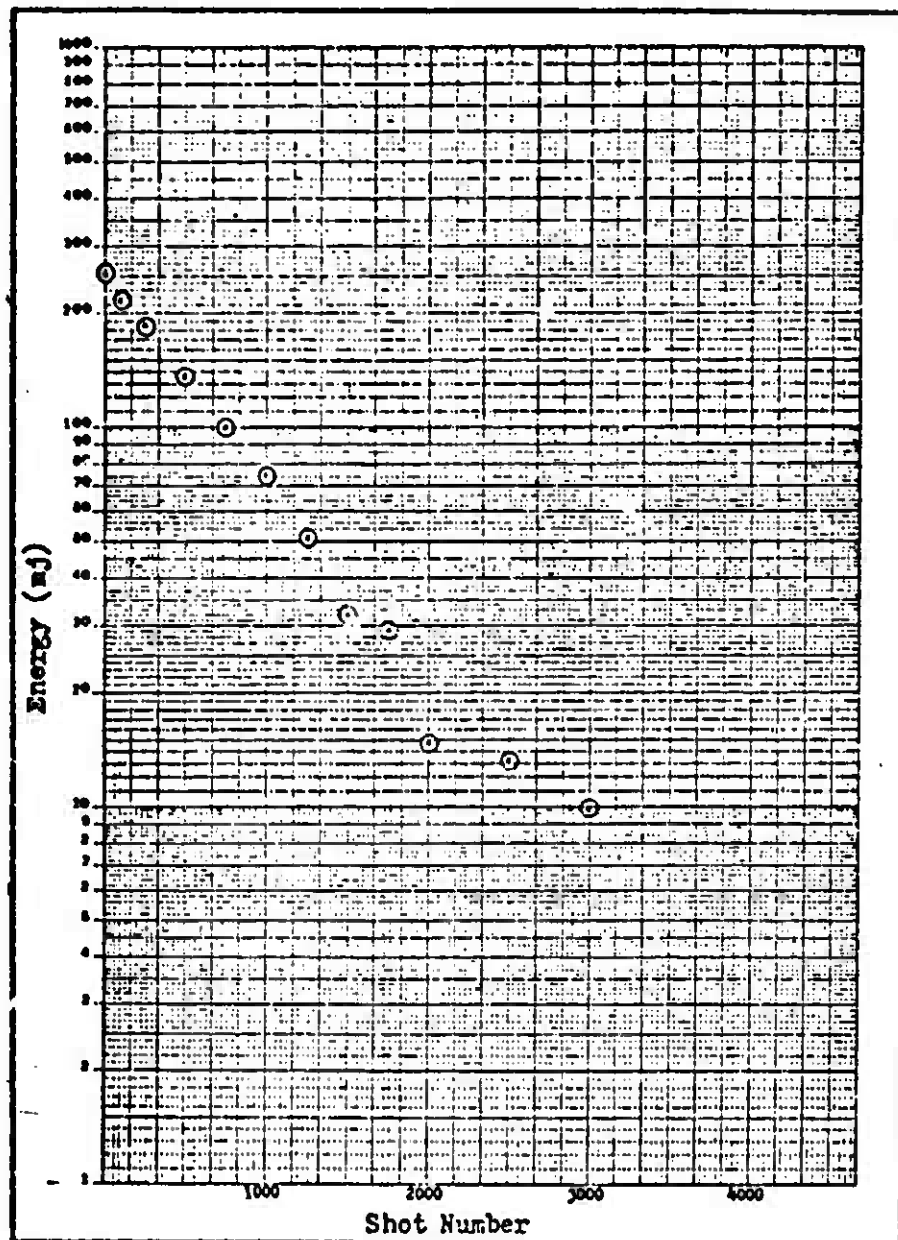Dye Concentration Versus Shot Number

for Trial 1

Figure E-2

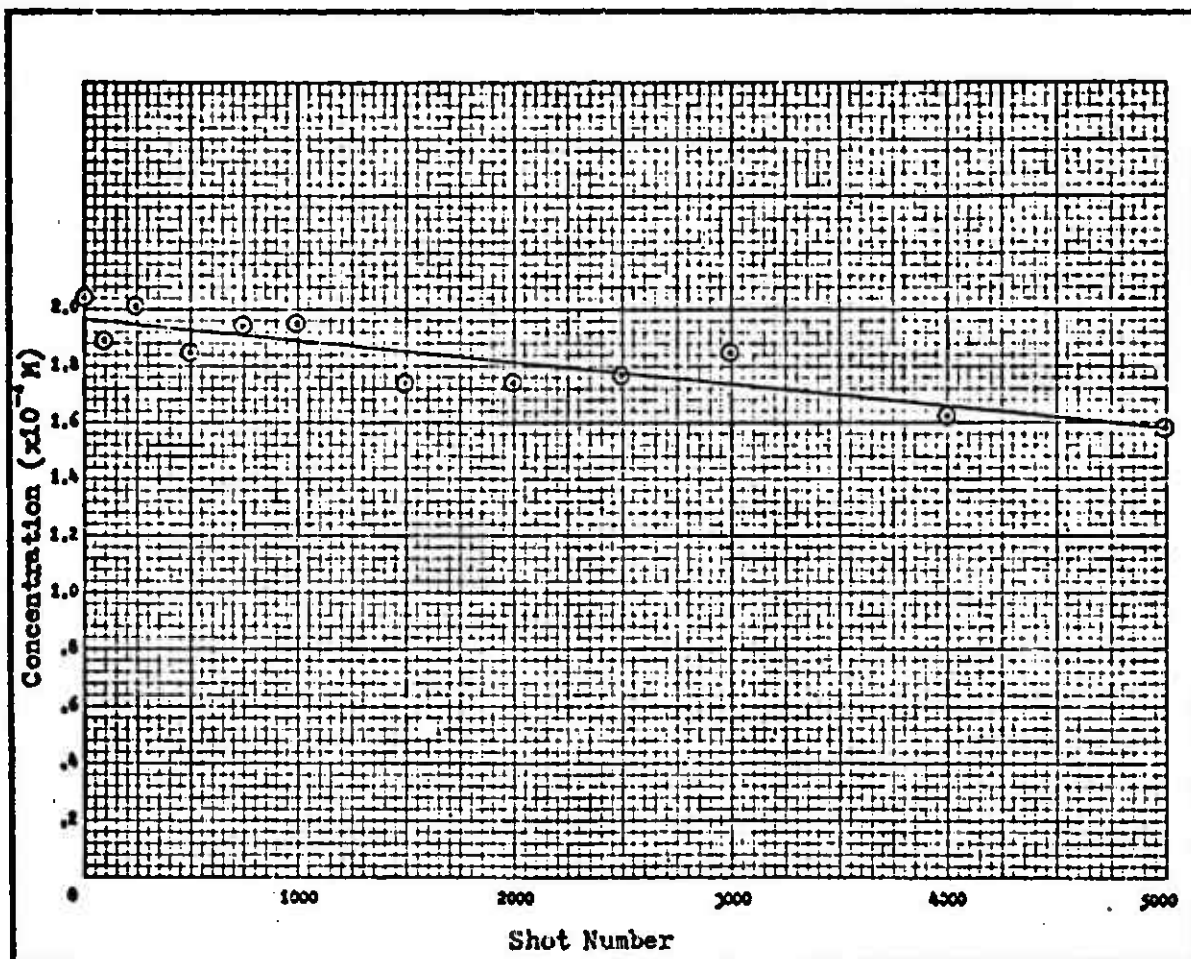Laser Energy Versus Shot Number

for Trial 1

82

Figure E-3

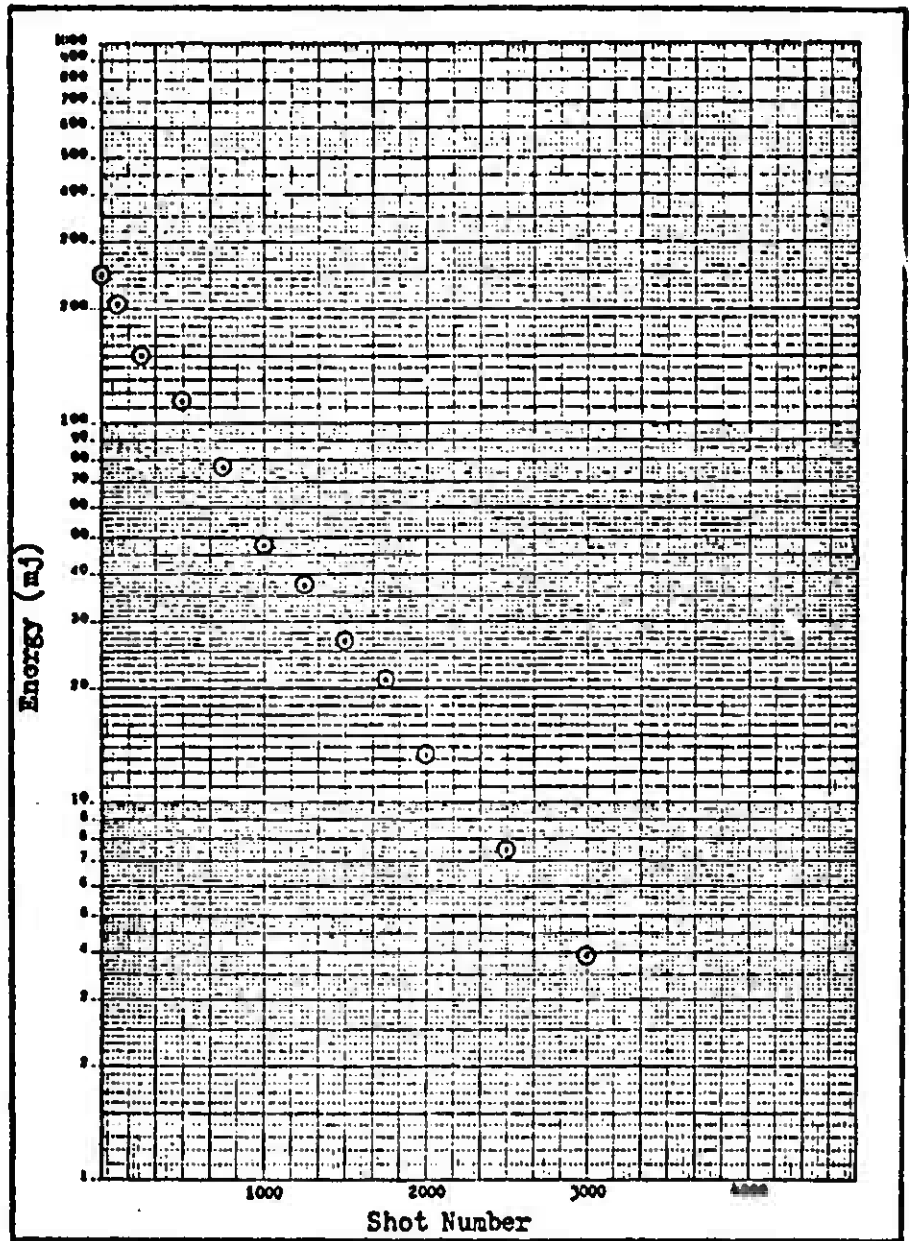Dye Concentration Versus Shot Number

for Trial 2
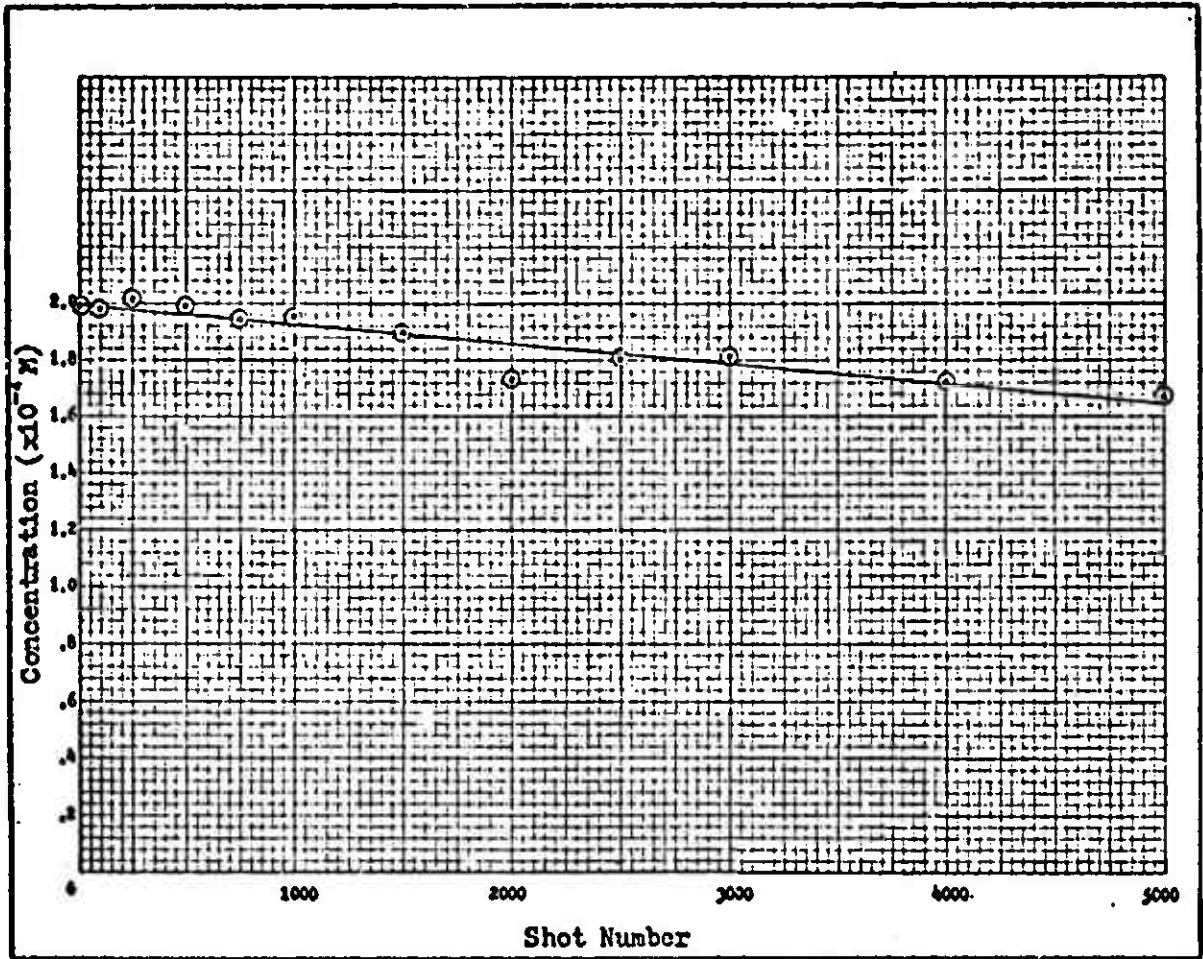
Figure E-4

Laser Energy Versus Shot Number

for Trisl 2

84

Figure E-5

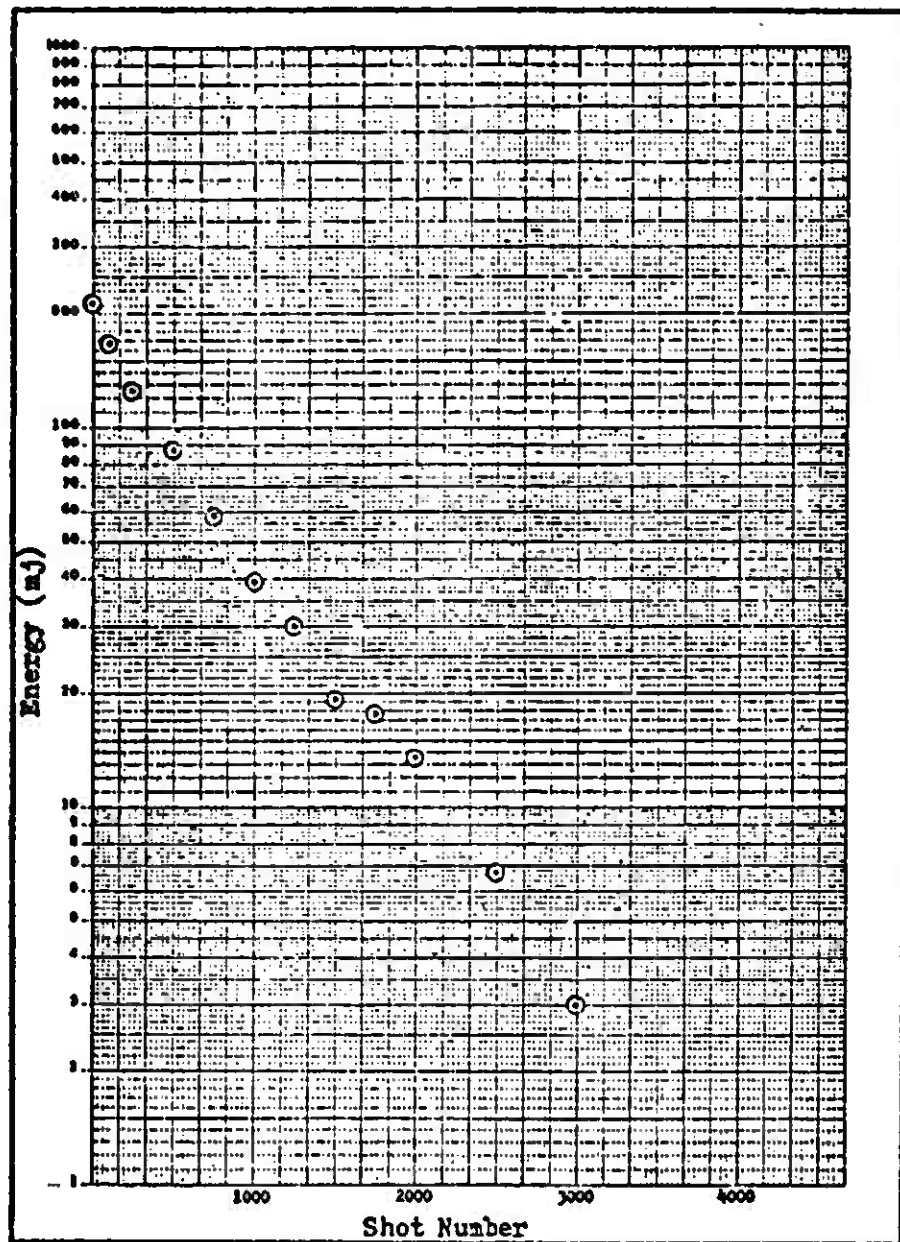Dye Concentration Versus Shot Number

for Trial 3

Figure E-6

Laser Energy Versus Shot Number

for Trial 3

86

Appendix F

Estimation of W_{max}

The flashlamp in the dye laser used to obtain the degradation data produced a spectrum comparable to a 25,000-degree Kelvin (°K) blackbody. The voltage (V) across the capacitor bank immediately before the laser was pulsed was 18 kilovolts (Ref 25:16, 21). The capacitance (C) was 0.329 microfarads (Ref 26:12). The total energy expended by the capacitor (E_T) into the flashlamp was then

$$E_T = \frac{1}{2} CV^2 = \frac{1}{2}(0.329 \times 10^{-6} f)(18 \times 10^3 V) = 53.3 \text{ joules} \qquad \text{(F.1)}$$

The efficiency of the flashlamp is assumed to be 20% (Ref 26:13); this puts the energy output of one flashlamp pulse at 10.7 joules. Figure 14 shows the visible spectrum for the dye solution. The 460-600 nm peak corresponds to the $S_0 \rightarrow S_1$ fundamental transition absorption. The part of the total energy in the pulse that is within this band can be determined using blackbody radiation tables (Ref 24:229-230). By interpolating the figures given for 24,000°K and 26,000°K blackbodies, we find that 0.03 or 3% of the total energy of the pulse lies within this band. As indicated by the spectrum, not all of this energy will actually be absorbed by the dye solution, but additional energy from the pulse will be absorbed in overtone transitions. Considering the gain from the overtone bands to offset the losses in the fundamental band, the energy absorbed by the medium is (10.7 j)(0.03) = 0.32 joules. For the Gaussian distribution pumping function, we can estimate W_{max} by solving the integral equation

87

$$\int_{-T}^{T} W_{max} \exp\left[-\ln 2 \ (t^2/T^2)\right] dt = 0.32 \text{ joules} \qquad (F.2)$$

Eq (F.2) can alternately be expressed by Eq (F.3):

$$W_{max} = \frac{0.32 \text{ joules}}{2\int_{0}^{T} \exp\left[-\ln 2 \ (t^2/T^2)\right] dt} \qquad (F.3)$$

To determine this integral the following approximation is made:

$$\int_{0}^{T} \exp\left[-\ln 2 \ (t^2/T^2)\right] dt \simeq \int_{0}^{\infty} \exp\left[-\ln 2 \ (t^2/T^2)\right] dt \qquad (F.4)$$

The average duration of the flashlamp pulse was 500 nanoseconds (Ref 25:16). Setting $T = 250 \times 10^{-9}$ sec, we can now solve Eq (F.3) using definite intergral tables (Ref 7:426) to get $W_{max} = 6 \times 10^5$ joules/sec. Selecting 540 nm as the average pump photon wavelength, W_{max} can be expressed in photons/sec:

$$W_{max} = (6 \times 10^5 \text{j/sec}) \frac{540 \times 10^{-7} \text{ cm}}{(3 \times 10^{10} \text{cm/sec})(6.63 \times 10^{-34} \text{j/sec})}$$

$$= 1.6 \times 10^{24} \text{ photons/sec} \qquad (F.5)$$

Vita

Alan J. Briding

attended the United States Air Force Academy. He graduated on 6 June, 1973 with a Bachelor of Civil Engineering and received his commission in the USAF. He went through undergraduate pilot training at Reese AFB, Texas and received his wings in September 1974. He then served as a C-141 aircraft commander and flight instructor in the 14th Military Airlift Squadron, 63rd Military Airlift Wing at Norton AFB, California until entering the School of Engineering, Air Force Institute of Technology, in June 1979.

REPORT DOCUMENTATION PAGE		READ INSTRUCTIONS BEFORE COMPLETING FORM
1. REPORT NUMBER AFIT/GEP/PH/80D-1	2. GOVT ACCESSION NO. AR-A094 417	3. RECIPIENT'S CATALOG NUMBER
4. TITLE *(and Subtitle)* ANALYSIS OF DYE DEGRADATION EFFECTS ON OUTPUT ENERGY OF THE PULSED ORGANIC DYE LASER		5. TYPE OF REPORT & PERIOD COVERED MS Thesis
		6. PERFORMING ORG. REPORT NUMBER
7. AUTHOR(s) Alan J. Briding Capt		8. CONTRACT OR GRANT NUMBER(s)
9. PERFORMING ORGANIZATION NAME AND ADDRESS Air Force Institute of Technology (AFIT-EN) Wright-Patterson AFB, Ohio 45433		10. PROGRAM ELEMENT, PROJECT, TASK AREA & WORK UNIT NUMBERS
11. CONTROLLING OFFICE NAME AND ADDRESS		12. REPORT DATE December 1980
		13. NUMBER OF PAGES 91 Pages
14. MONITORING AGENCY NAME & ADDRESS*(if different from Controlling Office)*		15. SECURITY CLASS. *(of this report)* Unclassified
		15a. DECLASSIFICATION/DOWNGRADING SCHEDULE

16. DISTRIBUTION STATEMENT *(of this Report)*

Approved for public release; distribution unlimited.

17. DISTRIBUTION STATEMENT *(of the abstract entered in Block 20, if different from Report)*

18. SUPPLEMENTARY NOTES

06 JAN 1981

Approved for Public Release; IAW AFR 190-17

FREDERICK C. LYNCH, Major, USAF
Director of Public Affairs

19. KEY WORDS *(Continue on reverse side if necessary and identify by block number)*
Dye Laser, KRS, Rate Equations, Reaction Products, Dye Degradation, Pulsed Laser, Dye Degradation Effects, Multiplier Effect

20. ABSTRACT *(Continue on reverse side if necessary and identify by block number)*
The dominant excitation and relaxation mechanisms found in dye molecules are discussed and then incorporated into a model for the xanthene dye laser. Rate equations for this model are presented which include terms that account for excited state singlet absorption and triplet absorption. The system of rate equations are solved using the steady-rate approximation to derive equations for the threshold pump power and output power of the laser.
The output power and threshold pump power equations are modified to include variables that allow the following effects of dye degradation to be examined:

DD FORM 1473 EDITION OF 1 NOV 65 IS OBSOLETE

dye concentration reduction, reaction product absorption of pump radiation, reaction product absorption of laaing radiation, and singlet quenching by the reaction products. Theoretical values based on available experimental data are derived for these variables. A computer program is used to integrate the output power of the laser over the duration of a flashlamp pulse to compute the pulse energy. The energy decay curves computed using the theoretical data are presented and compared to the experimental pulse energy decay.